Axially Chiral Catenanes and π-Electron-Deficient Receptors**

Masumi Asakawa, Peter R. Ashton, Sue E. Boyd, Christopher L. Brown, Stephan Menzer, Dario Pasini, J. Fraser Stoddart,* Malcolm S. Tolley, Andrew J. P. White, David J. Williams, and Paul G. Wyatt

Abstract: The design of a new class of chiral [2]catenanes is reported. The self-assembly of [2]catenanes comprising one or two 3,3′-bitolyl spacers in the π-electron-deficient component, and bis-*p*-phenylene-34-crown-10 (**BPP34C10**) as the π-electron-rich component, is described. The X-ray crystal structures, together with solution-state dynamic ^{1}H NMR spectroscopic studies, show that the degree of order characterizing the molecular structures is substantially different from that of the "parent" [2]-catenane, comprising cyclobis(paraquat-*p*-phenylene) and **BPP34C10**. When appropriately substituted in their *ortho* positions, bitolyl compounds can support axial chirality: the self-assembly of axially chiral [2]catenanes, comprising one or two 3,3′-disubstituted-2,2′-dihydroxy-1,1′-binaphthyl spacers, has been achieved in good yields, showing that the introduction of the bulky, axially chiral spacer and the consequent distortion of the cavity of the π-electron-deficient component still permits good molecular recognition between the components leading to efficient catenane production. X-ray crystallography suggests that this recognition is driven by hydrogen bonding and π–π stacking interactions between the complementary subunits. The hydroxyl groups on the chiral spacer were further functionalized as benzoyl esters in a [2]catenane as well as in the tetracationic cyclophanes; that is, chemistry can be done on these catenanes. The chiral tetracationic cyclophanes exhibit good enantiomeric differentiation toward the D- and L-enantiomers of aromatic amino acids in water and their *N*-acetylated derivatives in organic solvents.

Keywords
catenanes · chirality · enantioselection · receptors · self-assembly

Introduction

Self-assembly[1] is a very powerful tool for the construction of highly ordered supramolecular systems like those found in the natural world: the building of thermodynamically stable structures such as DNA,[2] the tobacco mosaic virus,[3] and many multimeric proteins[4] are all striking examples of the remarkable efficiency of self-assembly processes. An increasing number of abiotic self-assembling systems have been reported recently in the literature, for example, double-stranded helicates,[5] interlocked systems,[6] hydrogen-bonded aggregates,[7] and Langmuir–Blodgett films.[8] Recently, we have developed an approach (Figure 1) to mechanically interlocked molecular structures, based on a self-assembly paradigm and with subunits possessing high complementarity.[9] The strong molecular recognition that exists between the π-electron-deficient cyclobis(paraquat-*p*-phenylene) ($\mathbf{1}^{4+}$) and π-electron-rich macrocyclic polyether components, like 1,4-bis[2-(2-hydroxyethoxy)-ethoxy]benzene (**BHEEB**), is a result of hydrogen bonding[10] and dispersive interactions, including π–π stacking interactions;[11] the same kind of interactions are responsible for the molecular recognition that occurs between the π-electron-rich crown ether, bis-*p*-phenylene-34-crown-10 (**BPP34C10**), and paraquat (**PQT**). These interactions provide the key to our particular approach to the construction of interlocked compounds such as the [2]catenane $\mathbf{2}^{4+}$.[12] The remarkable ability of cyclobis(paraquat-*p*-phenylene) ($\mathbf{1}^{4+}$) to form stable inclusion complexes with biologically important compounds (e.g., amino acids possessing π-electron-rich aromatic subunits,[13a] a series of catechol-containing neurotransmitters,[13b] and phenyl glycopyranosides[13c]) led us to consider the possibility of introducing chirality into the cyclophane component and so render it a chiral π-electron-deficient receptor.[14] Furthermore, chiral [2]catenanes are of interest in the field of topological stereo-

[*] Prof. J. F. Stoddart, Dr. M. Asakawa, Dr. S. E. Boyd, Dr. C. L. Brown, P. R. Ashton, D. Pasini, M. S. Tolley
School of Chemistry, University of Birmingham
Edgbaston, Birmingham B15 2TT (UK)
Fax: Int. code +(121)414-3531
Prof. D. J. Williams, Dr. S. Menzer, Dr. A. J. P. White
Chemical Crystallography Laboratory, Department of Chemistry
Imperial College, South Kensington, London SW7 2AY (UK)
Fax: Int. code +(171)594-5804
Dr. P. G. Wyatt
Glaxo-Wellcome Medicines Research Centre, Gunnels Wood Road
Stevenage, Hertfordshire SG1 2NY (UK)
Fax: Int. code +(1438)763-352

[**] "Molecular Meccano", Part 16: for Part 15, see D. B. Amabilino, P. R. Ashton, S. E. Boyd, M. Gómez-López, W. Hayes, J. F. Stoddart, *J. Org. Chem.* **1997**, in press.

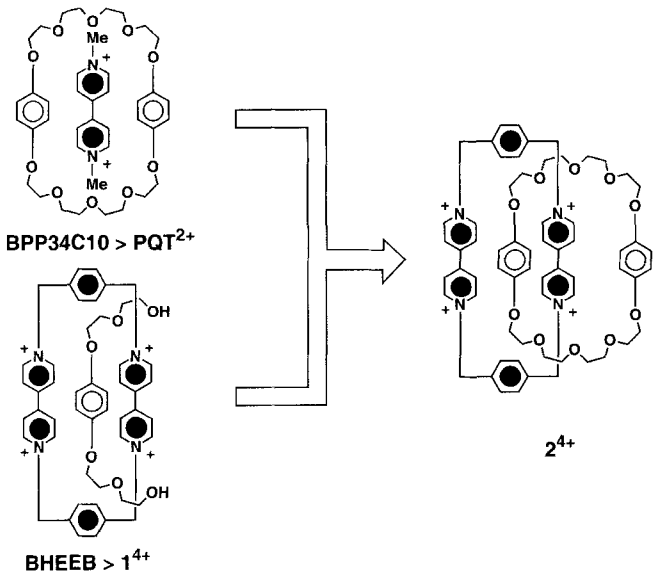

Figure 1. A self-assembly approach to mechanically interlocked compounds.

chemistry.[15, 16] Previously, we have synthesized an optically active [2]catenane $3\cdot4PF_6$ by substituting one of the *p*-xylyl spacers in the cyclobis(paraquat-*p*-phenylene) component with an optically active polyether chain incorporating a chiral hydrobenzoin unit (Scheme 1).[17] The corresponding optically active tetracationic cyclophane $4\cdot4PF_6$ was also prepared and characterized. Complexation studies between this cyclophane and π-electron-rich aromatic substrates, however, revealed only relatively weak binding with them.[18] These results might be rationalized in terms of the relative flexibility of the chiral spacer, resulting in a reduced level of preorganization of the host toward its potential guests. In order to build chirality into the receptor and also preserve its rigidity, we decided to introduce axial chirality. Initially, we considered 2,2′-bis(bromomethyl)-1,1′-binaphthyl ((*RS*)-**5**) as a chiral spacer to be inserted into a π-electron-deficient receptor. Previous studies had shown that reducing the width of the cavity of 1^{4+} by substituting one or both of its *p*-xylyl spacers with *m*-xylyl spacers still allows it to recognize π-electron-rich substrates and be incorporated into catenanes.[19] In this case, however, the desired [2]catenane (RS)-$9\cdot4PF_6$ could not be self-assembled as a result of attempted template-directed syntheses (Scheme 2), even under high-pressure reaction conditions. The reluctance of this collection of precursors to self-assemble into a [2]catenane was attributed to the fact that the tricationic intermediate probably prefers to undergo intermolecular nucleophilic substitution in preference to intramolecular ring closure—presumably as a consequence of the extreme narrowness of the cavity of the tetracationic cyclophane that would have to be formed. Thus, subsequent attempts to introduce axial chirality into the tetracationic cyclophane component centered on 3,3′-disubstituted-2,2′-

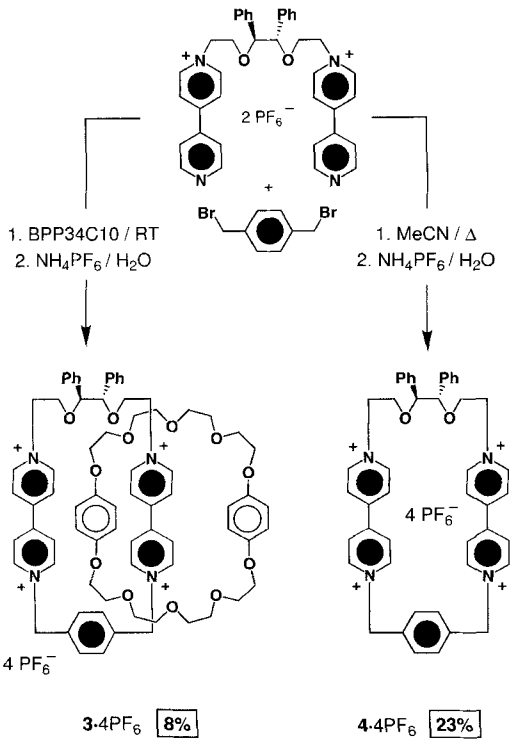

Scheme 1. The self-assembly of an optically active [2]catenane ($3\cdot4PF_6$) and the corresponding optically active cyclophane ($4\cdot4PF_6$).

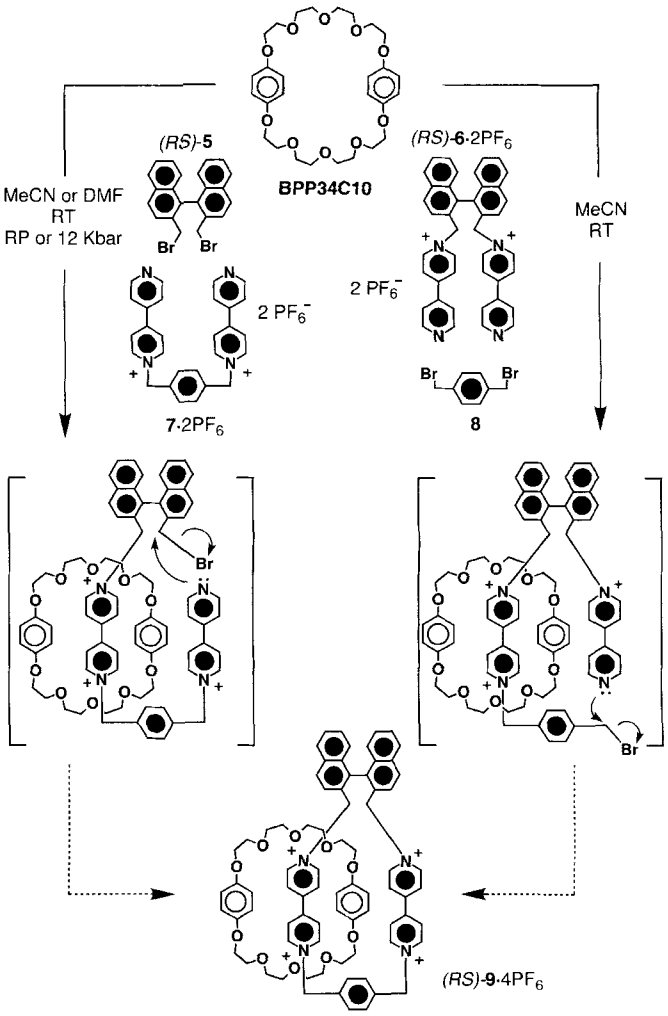

Scheme 2. Attempted self-assembly of the [2]catenane $9\cdot4PF_6$.

© VCH Verlagsgesellschaft mbH, D-69451 Weinheim, 1997 0947-6539/97/0303-0464 $ 15.00+.25/0 Chem. Eur. J. 1997, 3, No. 3

dihydroxy-1,1′-binaphthyl units. In this paper, we report on the design and the self-assembly of a new class of axially chiral [2]catenanes as well as on their tetracationic cyclophane components. We also examine the ability of the cyclophanes to differentiate between *enantiomers* of amino acids carrying π-electron-rich rings.[20]

Results and Discussion

Synthesis: 3,3′-Bis(bromomethyl)biphenyl (**10**) was prepared by a free-radical bromination of commercially available 3,3′-dimethylbiphenyl. Reaction of an excess of 4,4′-bipyridine with **10** yielded, after purification by column chromatography and counterion exchange, the dicationic intermediate **11**·2PF$_6$ in 47% yield. The [2]catenane **14**·4PF$_6$, incorporating one bitolyl spacer, has been self-assembled by means of both possible clipping procedures, following the two pathways shown in Scheme 3. Although the catenations were performed under identical conditions (solvent and temperature), when **10** was added to **7**·2PF$_6$ in the presence of an excess of **BPP34C10**, the [2]catenane **14**·4PF$_6$ was obtained in 33% yield, whereas, when the self-assembly was performed with equimolar amounts of 1,4-bis(bromomethyl)benzene **8** and **11**·2PF$_6$, the yield went up to 60%. Clearly, the intermediate tricationic complex **13**·3X undergoes ring closure much more readily than does **12**·3X.[19] Similarly, the [2]catenane **15**·4PF$_6$, incorporating two bitolyl spacers, has been self-assembled by the clipping procedure (see Scheme 4). Stirring **11**·2PF$_6$ and **10** in MeCN in the presence of an excess of **BPP34C10** at room temperature and pressure

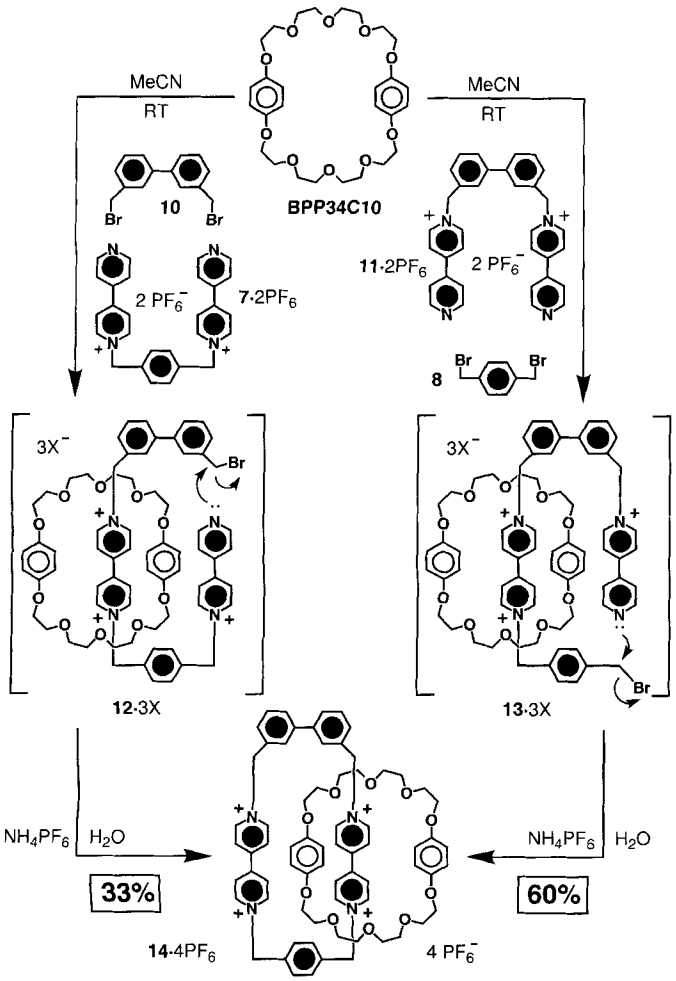

Scheme 3. The self-assembly of the [2]catenane **14**·4PF$_6$.

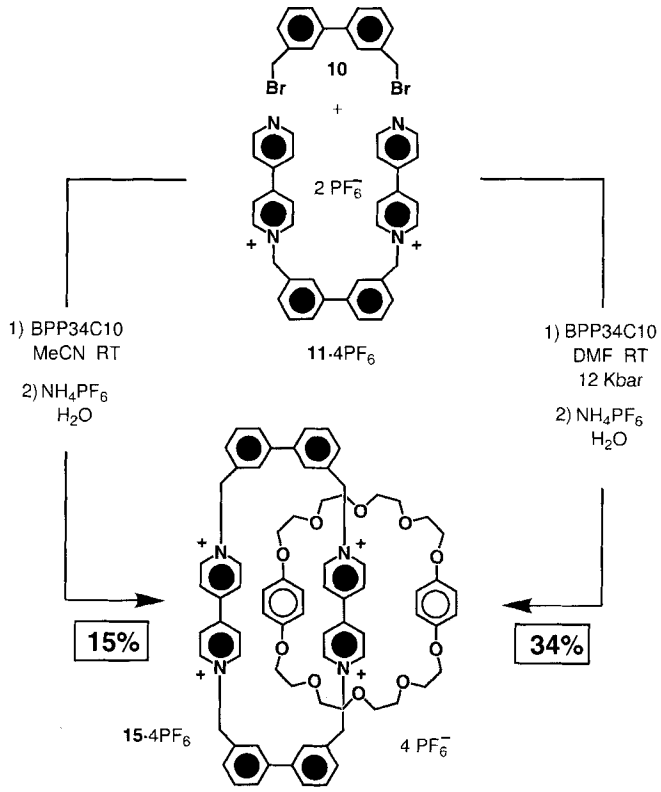

Scheme 4. The self-assembly of the [2]catenane **15**·4PF$_6$.

afforded **15**·4PF$_6$, after purification by column chromatography and counterion exchange, in 15% yield. When the reaction was carried out in DMF under high-pressure conditions the yield went up to 34%. No trace of the corresponding [3]catenane was detected, indicating that the cavity of the tetracationic cyclophane is too small to accommodate two **BPP34C10** hydroquinone rings simultaneously. This result contrasts with the case where 4,4′-bitolyl spacers are used in the π-electron-deficient component. In this case, the [3]catenane is the major product.[12c, 21] The syntheses of the free tetracationic cyclophanes have also been addressed. When equimolar amounts of **10** and **7**·2PF$_6$ were stirred at room temperature in dry MeCN, the tetracationic cyclophane **16**·4PF$_6$ was obtained (Scheme 5) in trace amounts. When the reaction was repeated under the same conditions in the presence of an excess of **BHEEB**, the yield increased to 14%, after purification by liquid–liquid extraction, column chromatography, and counterion exchange. The π-electron-rich hydroquinone ring and the hydrogen-bond-accepting oxygen atoms in **BHEEB** act as a template for the formation of the cyclophane in a procedure analogous to that for the template-directed synthesis of cyclobis(paraquat-*p*-phenylene).[12b] Likewise, the tetracationic cyclophane **17**·4PF$_6$ was obtained in 14% yield by stirring **10** and

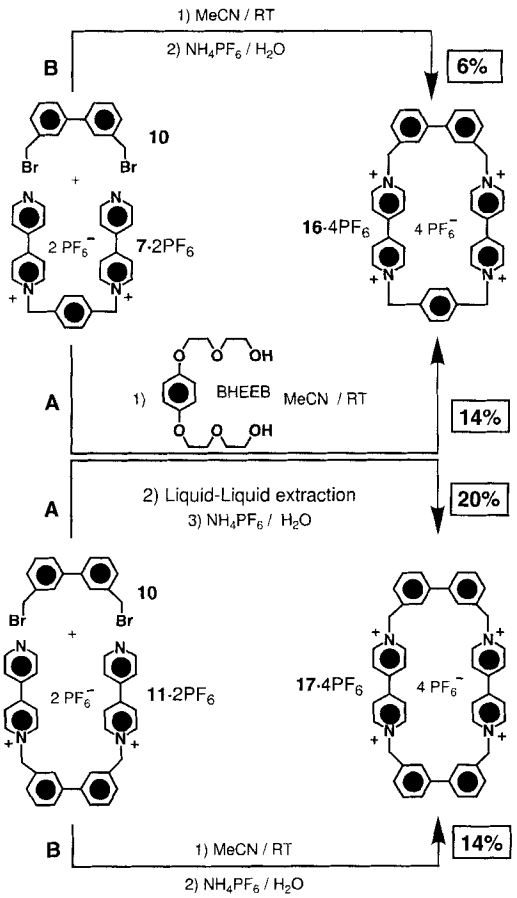

Scheme 5. The template-directed synthesis of the tetracationic cyclophanes **16**·4PF_6 and **17**·4PF_6.

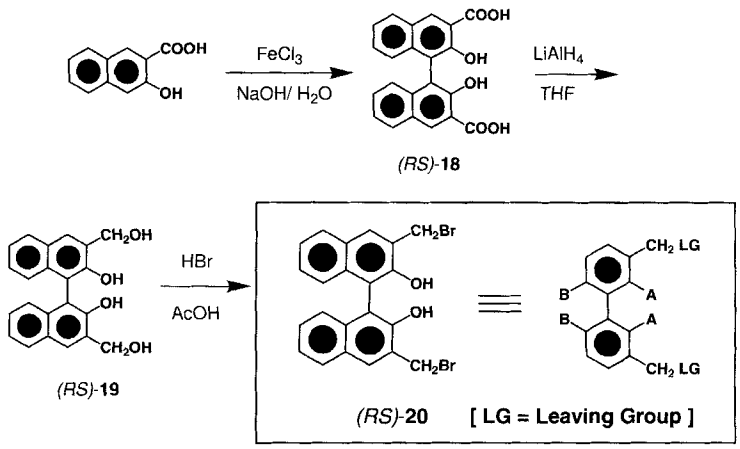

Scheme 6. Schematic representation and synthesis of the chiral building block (*RS*)-**20**.

bromination was achieved with HBr in $MeCO_2H$ at room temperature to give the racemic (*RS*)-3,3′-bis(bromomethyl)-2,2′-dihydroxy-1,1′-binaphthyl (*RS*)-**20** in 75% yield. When (*RS*)-**20** was stirred at room temperature in the presence of an equimolar amount of **7**·2PF_6 in dry MeCN and of an excess of **BPP34C10**, the chiral [2]catenane (*RS*)-**21**·4PF_6 self-assembled in 54% yield, following the usual purification procedures (Scheme 7). The much higher yield associated with the catenation step, when compared with that obtained from the self-assemby of the [2]catenane **14**·4PF_6, may be the consequence of at least two factors: a) the higher rigidity of the chiral spacer (*RS*)-**20** with respect to the flexible, achiral spacer **10** resulting in a higher preorganization toward ring closure, and b) the

11·2PF_6 in MeCN at room temperature, following the usual purification procedures.[22] Also, in this case, the use of the template raised the yield to 20%. This increase in the yield is less dramatic, presumably because the enlarged cavity of the tetracationic cyclophane diminishes its binding ability toward **BHEEB**. This observation is in line with the very poor templating power of polyether-substituted π-electron-rich aromatic units in the synthesis of cyclobis(paraquat-4,4′-biphenylene).[23]

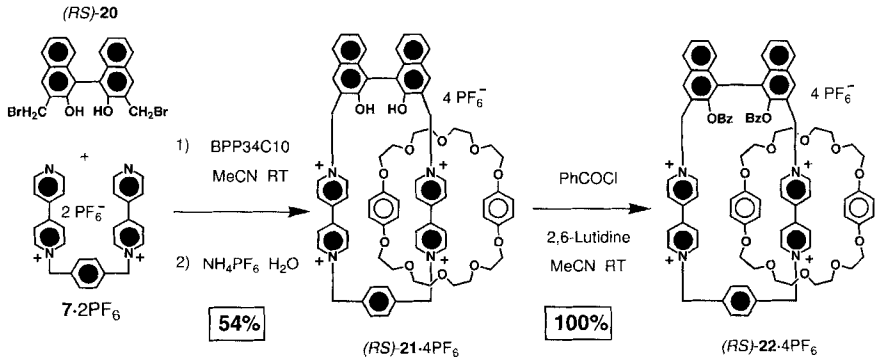

Scheme 7. The self-assembly of the chiral [2]catenane (*RS*)-**21**·4PF_6 and the synthesis of its derivative (*RS*)-**22**·4PF_6.

The strategy employed for the synthesis of a rigid, axially chiral spacer is shown in Scheme 6. The target compound should have leaving groups in the 3,3′ positions and bulky groups in the four 2,2′ and 6,6′ positions of the bitolyl skeleton in order to prevent racemization of the two enantiomers. The compound 3,3′-bis(bromomethyl)-2,2′-dihydroxy-1,1′-binaphthyl ((*RS*)-**20**) satisfies these criteria. Its synthesis and resolution have been reported by several research groups.[24] Cram and coworkers[25] have shown that it is stable toward racemization. The compound 2,2′-dihydroxy-1,1′-binaphthyl-3,3′-dicarboxylic acid (*RS*)-**18** could be obtained in modest yield by means of a free-radical reductive coupling of 3-hydroxy-2-naphthoic acid. The tetraol (*RS*)-**19** was obtained in good yields by reduction of the diacid with $LiAlH_4$. Finally, presence of the free hydroxyl groups in the binaphthyl unit, which might assist ring closure and hence [2]catenane formation by participating in hydrogen-bonding interactions with the polyether oxygen atoms of **BPP34C10**. The free hydroxyl groups in this interlocked structure could be functionalized. Indeed, the dibenzoate was formed when the [2]catenane (*RS*)-**21**·4PF_6 was stirred at room temperature in the presence of an excess of benzoyl chloride and 2,6-lutidine, affording (*RS*)-**22**·4PF_6 in quantitative yield (Scheme 7). This reaction, although it is a simple esterification, is the first example of the derivatization of an interlocked molecular system of this kind.

0947-6539/97/0303-0466 $ 15.00+.25/0 Chem. Eur. J. 1997, 3, No. 3

The synthesis of the optically active [2]catenane (*R*)-**22**·4PF$_6$ has also been addressed. The optical resolution of the chiral building block (*RS*)-**18** has been described in the literature by Cram and coworkers.[24c] When we employed the same procedure, based on the selective precipitation of one of the two diastereoisomeric salts formed by heating the racemic dicarboxylic acid (*RS*)-**18** with an excess of the optically active L-leucine methyl ester in MeOH, we obtained the optically active dicarboxylic acid (*R*)-**18**. The optically active dibromide (*R*)-**20** could be obtained by the strategy outlined for the racemic one. Although the optical rotation of the dibromide (*R*)-**20** has—to our knowledge—not been recorded in the literature (while the specific optical rotations of the diacid (*R*)-**18** and of the tetraol (*R*)-**19** have previously been described), we assumed that no racemization had occurred under the reaction conditions used in the bromination (slightly acidic conditions, 1 h, room temperature).[25] Stirring (*R*)-**20** in the presence of an equimolar amount of **7**·2PF$_6$ and an excess of **BPP34C10** in dry MeCN afforded the optically active [2]catenane (*R*)-**21**·4PF$_6$ in 50% yield, following the usual purification procedure. Stirring (*R*)-**20** and **7**·2PF$_6$ in the presence of the template **BHEEB**, followed by removal of the template by liquid–liquid extraction and purification by column chromatography before counterion exchange, gave the optically active π-electron-deficient tetracationic cyclophane (*R*)-**23**·4PF$_6$ in 27% yield (Scheme 8). Again, dibenzoylation of the hydroxyl groups on the cyclophane was achieved with benzoyl chloride and 2,6-lutidine, affording (*R*)-**24**·4PF$_6$ in 64% yield.

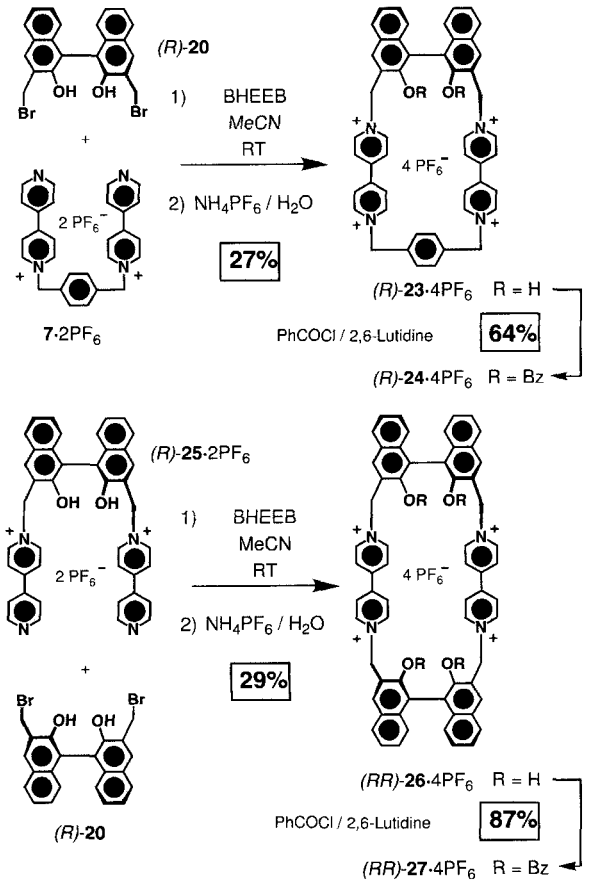

Scheme 8. The template-directed synthesis of the optically active tetracationic cyclophanes (*R*)-**23**·4PF$_6$ and (*RR*)-**26**·4PF$_6$.

Encouraged by the successful self-assembly of the tetracationic cyclophane and [2]catenane incorporating two achiral bitolyl units, we decided to investigate the possibility of introducing two chiral axes into the π-electron-deficient component. The dicationic salt (*R*)-**25**·2PF$_6$ was obtained in 44% yield (following purification by column chromatography and counterion exchange) by treating an excess of 4,4′-bipyridine with (*R*)-**20**. The self-assembly of the cyclophane (*RR*)-**26**·4PF$_6$, incorporating two axially chiral spacers, was achieved in 29% yield (Scheme 8) by allowing approximately equimolar amounts of (*R*)-**20** and (*R*)-**25**·2PF$_6$ to react in the presence of an excess of the template **BHEEB** at room temperature for 14 days before the usual purification procedures. Again, further functionalization of the four hydroxyl groups on the positively charged cyclophane was conducted, affording (*RR*)-**27**·4PF$_6$ in 87% yield. Intriguingly, the attempted self-assembly of (*RR*)-**28**·4PF$_6$ by reaction of (*R*)-**20** and (*R*)-**25**·2PF$_6$ in the presence of an excess of **BPP34C10** (Scheme 9) afforded the [2]catenane only in traces

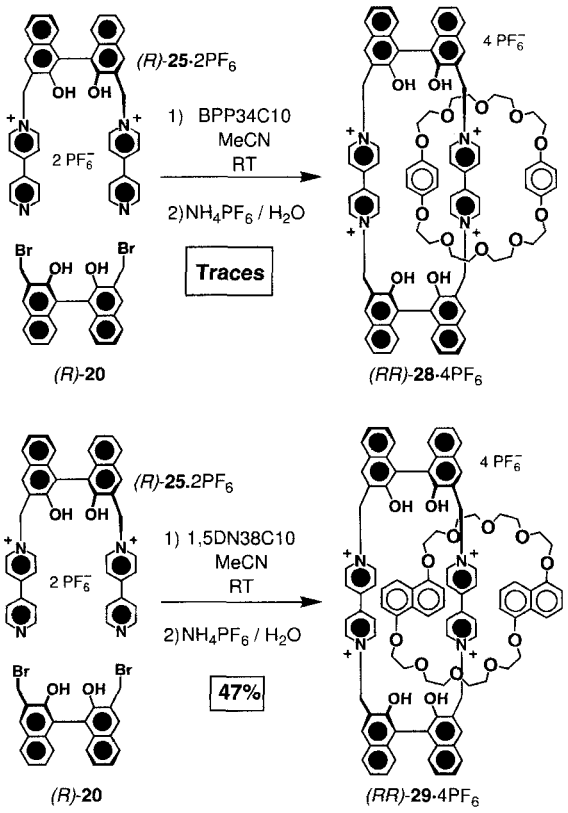

Scheme 9. The self-assembly of the chiral [2]catenane (*RR*)-**28**·4PF$_6$ and (*RR*)-**29**·4PF$_6$.

(identified by FAB mass spectrometry). Indeed, when the larger 1,5-dinaphtho-38-crown-10 (**1,5DN38C10**)[26] was used in the catenation, the appearance of a purple coloration in the reaction mixture was observed after a few hours and the [2]catenane (*RR*)-**29**·4PF$_6$ could be isolated after 14 days' stirring at room temperature, followed by the usual purification procedures, in 47% yield. Even although 1,5-dioxynaphthalene units are known to be better templating units for the self-assembly of interlocked compounds of this kind,[27] the association constant (K_a = 2510 M^{-1}, ΔG° = −4.7 kcal mol^{-1}) for the 1:1 complex

formed between (*RR*)-**26**·4PF$_6$ and **BHEEB** is certainly higher than the association constant ($K_a = 330\,M^{-1}$, $\Delta G^\circ = -3.45$ kcal mol^{-1}) for the 1:1 complex formed between (*RR*)-**26**·4PF$_6$ and 1,5-bis[2-(2-hydroxyethoxy)ethoxy]naphthalene **BHEEN**.[28] The very low yield (< 5%) of the [2]catenane (*RR*)-**28**·4PF$_6$ might be explained on the basis of steric interactions: the crown ether **BPP34C10** is too small in size to slip over the bulky binaphthol spacers once the tricationic intermediate—the product of the first nucleophilic substitution on one of the pyridyl nitrogen atoms of (*R*)-**25**·2PF$_6$ with one of the bromides of (*R*)-**20**—is formed, and hence is unable to encircle the newly formed bipyridinium unit. Thus, it appears that only with a larger crown ether such as **1,5DN38C10** can the self-assembly process work efficiently.[29]

X-Ray Crystallography: The X-ray analysis of the [2]catenane **14**·4PF$_6$ (Figure 2) reveals a structure in which one of the hydroquinone rings of the **BPP34C10** component is inserted

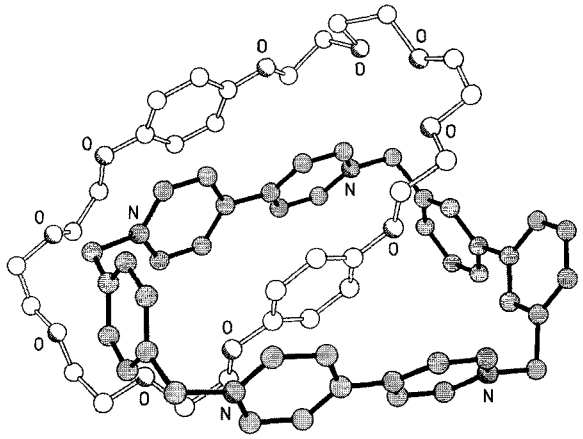

Figure 2. X-Ray crystal structure of the [2]catenane **14**·4PF$_6$.

approximately symmetrically through the center of the tetracationic cyclophane component, which consists of one bitolyl, one *p*-xylyl, and two bipyridinium units. The tetracationic cyclophane exhibits deformation characteristics analogous to those observed in cyclobis(paraquat-*p*-phenylene).[12b] There are twisting and bowing distortions within the two bipyridinium components, with twist and bow angles of 23° and 11°, respectively, for the "inside" bipyridinium unit, and 20° and 12° for the "alongside" one. The bitolyl unit, which adopts an *anti* geometry, also exhibits a large twist angle (49°) between its two phenylene rings. Associated with the *anti* geometry of the bitolyl unit, there is a significant tilting (24°) of the bond linking its two phenylene rings with respect to the $CH_2-C_6H_4-CH_2$ axis of the *p*-xylyl spacer at the other end of the cyclophane. The presence of a bitolyl spacer unit within the tetracationic cyclophane component increases the separation of the bipyridinium units to 7.5 Å (the mean value for cyclobis(paraquat-*p*-phenylene) (**1**$^{4+}$) is 7.1 Å),[12b] while the length of the tetracationic cyclophane, that is, the distance between the centroid of the *p*-xylyl spacer and the center of the bond linking the two phenylene rings of the bitolyl unit, is 11.2 Å. One of the effects of increasing the length of the spacer between the bipyridinium units of the cyclophane is an increase in the separation of the "inside" π-electron-rich hydroquinone ring and the two π-electron-deficient bipyridinium units. The distance of the hydroquinone ring to the "inside" bipyridinium unit is 3.68 Å and that to the "alongside" bipyridinium unit is 3.74 Å; in other words, it is only slightly displaced with respect to the central axis of the tetracationic cyclophane. The $O-C_6H_4-O$ axis of the "inside" hydroquinone ring (which has an *anti* geometry associated with its two oxymethylene bonds) is inclined by 40° to the plane of the cyclophane, as defined by the plane of its four methylene carbon atoms, which are coplanar to within 0.3 Å. The "alongside" hydroquinone ring, which has a predominantly *syn* geometry associated with its oxymethylene bonds (see the Experimental Section), is inclined by 19° to the plane of the cyclophane and has a separation of 3.56 Å from the "inside" bipyridinium unit. In addition to the π–π stabilizing interactions between the π-electron-rich hydroquinone rings and π-electron-deficient bipyridinium units, there are also weak [CH···O] hydrogen bonds involving α-CH groups on each ring of the "inside" bipyridinium unit and either the second or the third oxygen atom of each of the polyether linkages in the **BPP34C10** component. These interactions are very weak, with [H···O] distances in the range 2.49–2.56 Å and associated [CH···O] angles ranging between 140 and 149°. In contrast to the pattern observed in [2]catenanes, where the tetracationic cyclophane component is cyclobis(paraquat-*p*-phenylene) and there are strong T-type edge-to-face interactions between the "inside" hydroquinone ring and the *p*-xylyl spacers of the cyclophane, here, in **14**·4PF$_6$, this type of interaction appears to be absent. The centroid–centroid separation between the "inside" hydroquinone ring and the *p*-xylyl ring is 5.52 Å with an associated [H···π] distance of 3.4 Å—a distance that is very much longer than the normal value of ≈2.8 Å associated with a significant interaction.[12b] Inspection of the packing of the [2]catenane molecules of **14**·4PF$_6$ in the crystals (Figure 3) reveals the presence of a mosaic-like array of [2]catenane molecules. This array is stabilized by π–π interactions between a) the "alongside" hydroquinone ring of one molecule and one of the phenylene rings of the bitolyl unit of another (centroid–

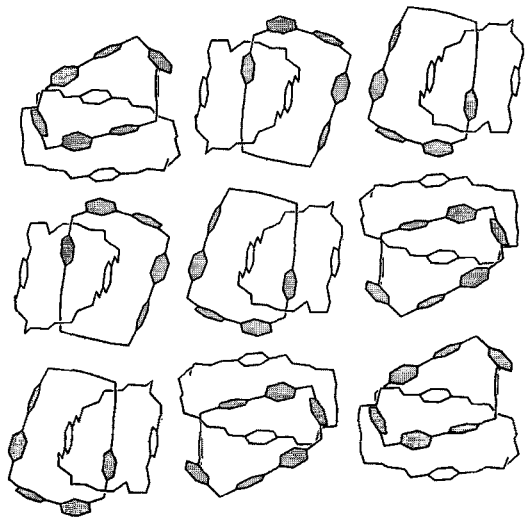

Figure 3. Packing of the molecules of the [2]catenane **14**·4PF$_6$ in the solid state.

0947-6539/97/0303-0468 $ 15.00+.25/0 Chem. Eur. J. 1997, 3, No. 3

centroid separation 3.93 Å, mean interplanar separation 3.59 Å, ring–ring tilt 11°) and b) one of the pyridinium rings of a bipyridinium unit in one molecule and its parallel-aligned centrosymmetrically related counterpart in another (centroid–centroid separation 4.40 Å, mean interplanar separation 4.12 Å). The apparent stacking geometry of *p*-xylyl rings in adjacent [2]catenanes (mean interplanar separation 3.18 Å, but with a centroid–centroid separation of 5.35 Å for the pairs of parallel rings) is not compatible with any significant π–π stacking interaction. These two-dimensional mosaics of [2]catenanes form sheets within the crystallographic 011 plane. Adjacent sheets are separated by a lattice translation (11 Å) in the *a* direction. The anions and solvent molecules are located between these layers.

The X-ray analysis of **15**·4PF$_6$ (Figure 4) reveals a [2]catenane structure very similar to that observed for the previous one (**14**·4PF$_6$) in that one of the hydroquinone rings of the

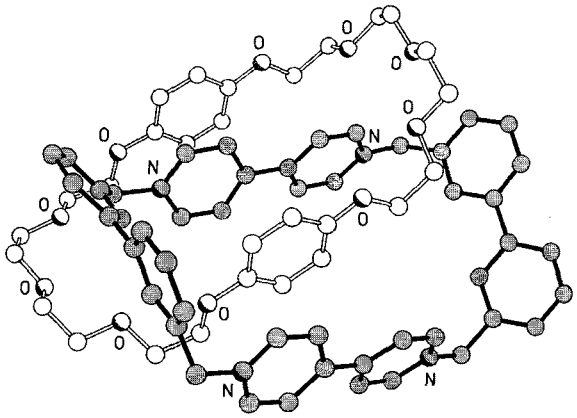

Figure 4. X-ray crystal structure of the [2]catenane **15**·4PF$_6$.

BPP34C10 component (which in **15**·4PF$_6$ has a *syn* relationship associated with its two oxymethylene bonds) is threaded approximately centrally through the cavity of the tetracationic cyclophane with its O–C$_6$H$_4$–O axis inclined by 41° to the plane of the cyclophane. The presence of two bitolyl spacer units within the tetracation results in an increase in its length to 12.8 Å (11.2 Å in **14**·4PF$_6$). Surprisingly, however, there is a small reduction in its width (between the two bipyridinium units) to 7.1 Å (7.5 Å in **14**·4PF$_6$). This reduction is probably a consequence of the adoption by both the bitolyl units of a *syn* geometry for each of their pairs of CH$_2$–Ar bonds, as opposed to the *anti* geometry adopted for the single bitolyl spacer in **14**·4PF$_6$. There are significant twists (12° and 30°) between the phenylene rings within each bitolyl unit. A consequence of the distinctly different twist angles in the two bitolyl spacers is a skewing of the overall geometry of the tetracationic cyclophane component, such that the [N···N] axes of the two bipyridinium units are inclined by 17°. The bipyridinium units both exhibit twisting and bowing distortions, with the "inside" one being twisted by 18° (14° bow) and with the "alongside" one also being twisted by 18°, but with only a 7° bow. It is interesting to note that the "inside" hydroquinone ring is offset quite markedly toward the bitolyl unit exhibiting the larger twist: the distance from the centroid of the hydroquinone ring to the center of the bond linking the two phenylene rings in one spacer is 5.6 Å, whereas it is 7.4 Å to the center of the bond of the other bitolyl unit (with the twist angle of 12°). The [2]catenane is stabilized by π–π interactions between the π-electron-rich hydroquinone rings and the π-electron-deficient bipyridinium units. The separation between the plane of the "inside" hydroquinone ring and the "alongside" bipyridinium unit is 3.54 Å, whereas its separation from the "inside" bipyridinium unit is 3.41 Å. The distance from the plane of the "alongside" hydroquinone ring (which also has a *syn* geometry for its oxymethylene bonds) and the "inside" bipyridinium unit is 3.63 Å. The O–C$_6$H$_4$–O axis of the "alongside" hydroquinone ring is inclined by 29° to the [N···N] axis of the "inside" bipyridinium unit. There is only one distinctive additional stabilizing interaction – that is a strong [CH···O] hydrogen bond ([C···O] 3.21 Å, [H···O] 2.28 Å, [CH···O] angle 165°) between one of the α-CH bipyridinium hydrogen atoms and the central polyether oxygen atom of one of the polyether linkages. The [2]catenane molecules pack to form extended π-donor/π-acceptor stacks (Figure 5) that

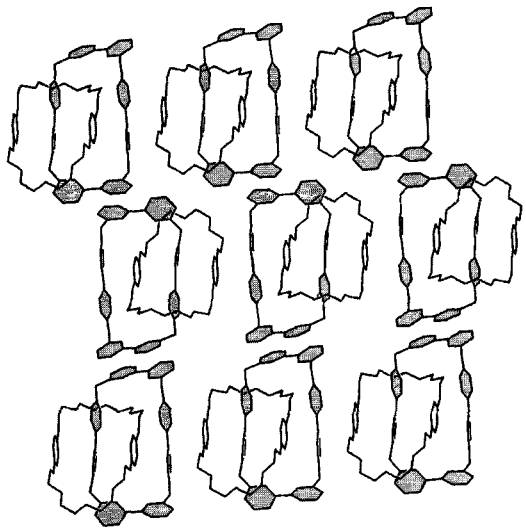

Figure 5. Packing of the molecules of the [2]catenane **15**·4PF$_6$ in the solid state.

extend in the crystallographic 1$\bar{1}$0 direction, the plane of the "alongside" hydroquinone ring in one molecule within the stack being separated by 3.49 Å from the "alongside" bipyridinium unit of the next. Adjacent centrosymmetrically related stacks in one direction are involved in interstack π–π interactions that occur between pairs of overlapping bitolyl units (ring-centroid–ring-centroid separations of 4.23 Å and mean interplanar separations of 3.77 Å). In the other direction, there is a similar interaction between stacks related by an independent crystallographic symmetry center, but offset such that only one of the phenylene rings of the other bitolyl unit is involved in parallel π–π overlap (interplanar separation 3.62 Å and centroid–centroid separation of 3.97 Å). The overall effect of these combined interactions is to produce once again a two-dimensional sheet mosaic, but with distinctive offsets between the individual components within the sheet. The anions and solvent molecules are located between the extended sheets of π–π stabilized [2]-catenane molecules.

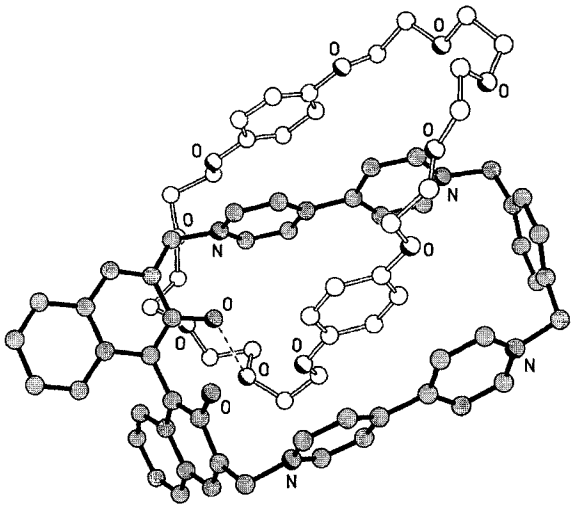

Figure 6. X-Ray crystal structure of the [2]catenane (*RS*)-**21**·4PF_6.

The X-ray analysis shows that the [2]catenane (*RS*)-**21**·4PF_6 crystallizes with equal numbers of (*R*) and (*S*) molecules present in the crystal. The **BPP34C10** component is threaded through the center of the chiral tetracationic cyclophane, with the O–C_6H_4–O axis of the "inside" hydroquinone ring inclined by 41° to the plane of the cyclophane, as defined by the four methylene carbon atoms that are coplanar to within 0.33 Å. The incorporation of the binaphthyl spacer into one of the arms of the tetracationic cyclophane noticeably reduces the amount of bowing in the bipyridinium units (typically ≈25–30°) usually present in this type of component to values of 4° for the "inside" bipyridinium unit and 9° for the "alongside" one. The twist angles, on the other hand, have typical values of 16° for the "inside" bipyridinium unit and 19° for the "alongside" one. The two naphthyl rings of the binaphthyl spacer are orthogonal to each other (twist angle 90°). Moreover, in contrast to cyclobis(paraquat-*p*-phenylene) and its related *m*-xylyl bridged analogues, where the geometries at the four corner methylene carbon atoms show little or no departure from tetrahedral,[12b, 19] in (*RS*)-**21**·4PF_6, the angles at the methylene junctions with the binaphthyl spacer are noticeably enlarged to 112 and 115°, while those associated with the *p*-xylyl spacer unit are unchanged at 108 and 109°. The length and breadth of the tetracationic cyclophane component (as defined by the distance from the center of the bond linking the two naphthyl rings to the centroid of the *p*-xylyl ring and the distance between the centers of the bonds linking each of the pyridinium rings within the bipyridinium units) are 11.6 and 7.2 Å, respectively. This [2]catenane is stabilized by π–π interactions between both the "inside" and the "alongside" π-electron-rich hydroquinone rings of the **BPP34C10** component and the proximal π-electron-deficient bipyridinium units of the tetracationic cyclophane component. The separations between the "inside" hydroquinone ring and the "inside" and "alongside" bipyridinium units are 3.61 and 3.53 Å, and the distance between the "alongside" hydroquinone ring and the "inside" bipyridinium unit is 3.50 Å. The O–C_6H_4–O axis of the "alongside" hydroquinone ring (which has a *syn* relationship associated with its phenoxymethylene bonds; compare this with the *anti* geometry characterizing the "inside" hydroquinone ring) is inclined by 32° to the [N···N] axis of the "inside" bipyridinium unit. Supplementing these interactions are both [OH···O] and [CH···O] hydrogen bonds between the tetracationic cyclophane component and oxygen atoms in the **BPP34C10** component. The strongest of these hydrogen-bonding interactions involves the inwardly directed hydroxyl group of the binaphthyl unit, which is within hydrogen-bonding distance of both the second (2.75 Å) and the third (2.87 Å) oxygen atoms in the proximal polyether chain of the **BPP34C10** component. Location of the hydroxyl hydrogen atom shows that the OH group is directed toward the second polyether oxygen atom; [H···O] distance is 2.23 Å (cf. 3.05 Å to the third oxygen atom), with an associated [OH···O] angle of 123°. Weaker hydrogen-bonding interactions exist between one of the "inside" α-CH bipyridinium hydrogen atoms (remote from the binaphthyl spacer) and the central oxygen atom of the polyether thread ([C···O] 3.39, [H···O] 2.46 Å; [CH···O] angle 163°) and also between one of the hydrogen atoms attached to the methylene carbon atom linking the "inside" bipyridinium unit and the binaphthyl spacer and the second oxygen atom of the polyether chain relative to the "alongside" hydroquinone ring ([C···O] 3.38, [H···O] 2.49 Å; [CH···O] angle 155°). In contrast to the majority of other [2]catenanes containing hydroquinone rings sandwiched between bipyridinium units within tetracationic cyclophane components containing *p*-xylyl spacers, in which T-type edge-to-face interactions between the inside hydroquinone ring and the *p*-xylyl rings are dominant, this type of interaction appears to be absent or very weak in (*RS*)-**21**·4PF_6. The centroid–centroid separation between the "inside" hydroquinone ring and the *p*-xylyl spacer is 5.42 Å, the *ortho* hydroquinone hydrogen atom being 3.25 Å from the *p*-xylyl ring centroid; a typical value is ≈2.8 Å. The probable reason for the absence of a T-type interaction is the fact that the hydroquinone ring is displaced toward the binaphthyl unit as a consequence of the presence of the strong [OH···O] hydrogen bond between one of the binaphthyl hydroxyl groups and an oxygen atom in the polyether linkage in the **BPP34C10** component. A study of the packing (Figure 7) of the [2]catenane molecules reveals an absence of any marked extended π–π stacking. Centrosymmetrically related pairs of [2]catenane molecules are oriented such that the outside hydroquinone rings of adjacent

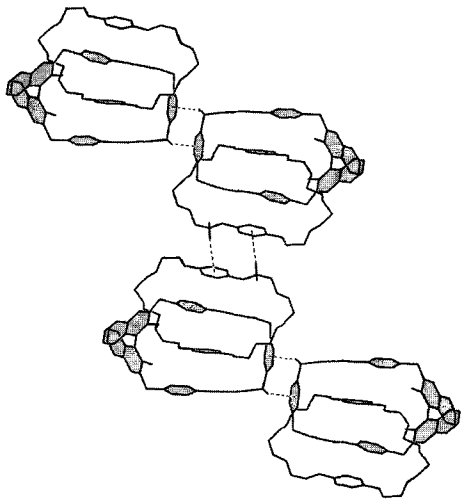

Figure 7. Packing of the molecules of the [2]catenane (*RS*)-**21**·4PF_6 in the solid state.

© VCH Verlagsgesellschaft mbH, D-69451 Weinheim, 1997 0947-6539/97/0303-0470 $ 15.00+.25/0 Chem. Eur. J. 1997, 3, No. 3

Table 1. Chemical shift data [δ values ($\Delta\delta$ values)] [a] obtained from the 400 MHz ^{1}H NMR spectra recorded for the series of [2]catenanes **2**·4PF$_6$, **14**·4PF$_6$, **15**·4PF$_6$ an the corresponding cyclophanes **1**·4PF$_6$, **16**·4PF$_6$, **17**·4PF$_6$ in CD_3COCD_3 solutions at room temperature.

Compound	Charged component				Neutral component
	α-CH	β-CH	C_6H_4 [b]	CH_2N^+	ArH
1·4PF$_6$ [c]	9.38	8.58	7.76	6.15	
16·4PF$_6$	9.52/9.39	8.64/8.59	7.78	6.19/6.16	
17·4PF$_6$ [d]	8.95	8.20		5.81	
2·4PF$_6$ [e]	9.28	8.18	8.04	6.01	6.28/3.78
	(−0.10)	(−0.40)	(+0.28)	(−0.14)	
14·4PF$_6$ [e]	9.34/9.13	8.15/8.10	8.02	6.11/6.09	6.23/4.66
	(−0.18/−0.26)	(−0.39/−0.49)	(+0.24)	(−0.08/−0.07)	
15·4PF$_6$ [d]	8.75	7.72		5.83	5.70
	(−0.20)	(−0.48)		(+0.02)	

[a] The $\Delta\delta$ values indicated in parentheses under the respective δ values relate to the changes in chemical shift exhibited by the probe protons upon catenane formation. negative value indicates a movement of the resonance to high field. [b] The C_6H_4 refers to the *p*-xylyl probe protons of the tetracationic cyclophane component. [c] Dat obtained from ref. [12c]. [d] Spectra recorded in CD_3CN. [e] Spectra recorded at 273 K.

Table 2. Kinetic and thermodynamic parameters[a] relating to the proposed processes 1 and 2 (Scheme 10) obtained from the temperature-dependent 400 MHz ^{1}H NM spectra recorded on the series of [2]catenanes **2**·4PF$_6$, **14**·4PF$_6$, **15**·4PF$_6$, and (*RR*)-**29**·4PF$_6$.

[2]catenane	Probe protons	$\Delta\nu$ [a] (Hz) ($\Delta\nu$) [b]	k_c [a] (s^{-1}) (k_{ex}) [b]	T_c [a] (K) (T_{ex}) [b]	$\Delta G_c^{\ddagger}$ [a] (kcal mol^{-1}) ($\Delta G_{ex}^{\ddagger}$) [b]	Process	Solvent
2·4PF$_6$	OC_6H_4O	(19)	(60)	(313)	(15.7)	1	CD_3CN
	α-CH	74	165	250	12.0	2	$(CD_3)_2CO$
	β-CH	34	76	247	12.2	2	$(CD_3)_2CO$
14·4PF$_6$	OC_6H_4O	(24)	(75)	(257)	(12.8)	1	$(CD_3)_2CO$
	α-CH	65	144	239	11.5	2	$(CD_3)_2CO$
	α'-CH	78	173	239	11.4	2	$(CD_3)_2CO$
15·4PF$_6$	OC_6H_4O	(24)	(75)	(230)	(11.4) [d]	1	$(CD_3)_2CO$
	α-CH	115	255	229	10.8	2	$(CD_3)_2CO$
	β-CH	84	187	230	11.0	2	$(CD_3)_2CO$
(*RR*)-**29**·4PF$_6$	$OC_{10}H_6O$	193	428	270	12.5	1	$(CD_3)_2CO$

[a] Data not in parentheses relate to the coalescence method (see ref. [30]). [b] Data in parentheses relate to the exchange method (see ref. [30]). [c] Data obtained fro ref. [12c]. [d] This data was calculated assuming $\omega_{1/2}$ to be 6 Hz in a situation of no exchange (see text).

molecules are aligned parallel and significantly offset with respect to each other (interplanar separation 4.04 Å, centroid–centroid separation 4.9 Å) at a distance that is somewhat large for any significant π-π interactions. However, one of the hydrogen atoms on an OCH_2 group in one molecule is directed into the face of the hydroquinone ring of another and vice versa, the [H···π] distance being 3.07 Å. A similar but stronger interaction also exists between parallel-aligned pairs of *p*-xylyl rings disposed about an independent crystallographic symmetry center. The interplanar separation is much smaller, at 3.22 Å, although the centroid–centroid separation is once again large (4.9 Å). This ring–ring offset is such that one of the *p*-xylyl methylene hydrogen atoms in one molecule is directed into the face of the *p*-xylyl ring of another and vice versa, the [H···π] distance being only 2.88 Å, with the [H···π] vector inclined by 76° to the *p*-xylyl ring plane. The combination of these [CH···π] interactions between [2]catenane molecules results in the formation of loosely linked zigzag chains of these molecules.

^{1}H NMR Spectroscopy: The solution-state properties of the series of [2]catenanes incorporating a π-electron-rich **BPP34C10** component and bearing one or two bitolyl spacers in their π-electron-deficient components have been investigated by means of variable-temperature ^{1}H NMR spectroscopy. The relevant chemical shift data are summarized in Table 1, and the associated kinetic and thermodynamic parameters for the dynamic processes (Scheme 10) taking place within these [2]catenanes are

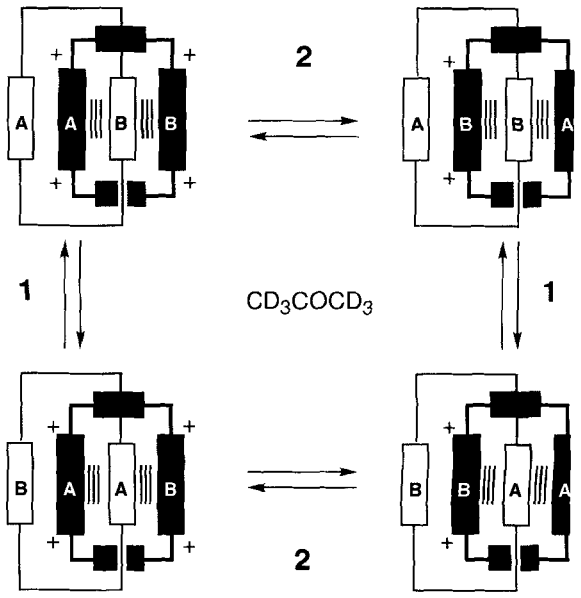

Scheme 10. The dynamic processes occurring in the [2]catenanes **14**·4P **15**·4PF$_6$, (*RS*)-**21**·4PF$_6$, and (*RR*)-**29**·4PF$_6$.

listed in Table 2.[30] The $\Delta\delta$ values exhibited by the protons the charged tetracationic cyclophane components of t [2]catenanes **14**·4PF$_6$ and **15**·4PF$_6$ are consistent with tho exhibited by the "parent" [2]catenane bearing two *p*-xylyl spa

ers, **2**·4PF$_6$; that is, a downfield shift is observed for the resonances attributable to the α protons of the bipyridinium moiety, a more pronounced shift being observed for the β protons. Upfield shifts are observed for the resonances of both the methylene bridges and the aromatic units of the spacer groups when compared with those observed for the free tetracationic cyclophanes **1**·4PF$_6$, **16**·4PF$_6$, and **17**·4PF$_6$. The kinetic and thermodynamic parameters (Table 2) for the passage of the **BPP34C10** component through the cavity of the tetracationic cyclophane components (process 1, Scheme 10) show that the activation barrier to this process is decreased upon introduction of one bitolyl spacer into the skeleton of the tetracationic cyclophane component. This trend continues as the cavity is further expanded by the introduction of a second bitolyl spacer. In fact, when both of the *p*-xylyl spacers in the tetracationic cyclophane component are substituted with bitolyl spacers, it is not possible to distinguish between the "inside" and "alongside" environments for the hydroquinone ring protons, even at temperatures as low as 200 K (400 MHz). An estimated value of the activation energy barrier for process 1 was obtained assuming the half-height linewidth ($\omega_{1/2}$) in absence of exchange to be less than 6 Hz, a typical value being 3 Hz.[30] The value obtained shows a decrease of more than 4 kcal mol^{-1} when compared with that obtained for the "parent" [2]catenane, **2**·4PF$_6$. This decrease in the activation barrier presumably reflects the reduced stability of the π-acceptor/π-donor/π-acceptor recognition motif in the catenane, as the bipyridinium acceptor units are held increasingly farther apart. In other words, the tetracationic cyclophane retains the π-electron-rich component less strongly in these systems. The circumrotation (process 2, Scheme 10) of the tetracationic cyclophane component through the cavity of the crown ether components, which leads to the exchange of the bipyridinium units A and B between positions "inside" and "alongside" the crown ether components, also occurs in the [2]catenanes. The activation energy barriers associated with process 2 could be obtained for both **14**·4PF$_6$ and **15**·4PF$_6$; these values show good agreement with that reported for the "parent" [2]catenane **2**·4PF$_6$.

The relevant chemical shift data for the series of [2]catenanes incorporating the chiral binaphthol spacers and the corresponding tetracationic cyclophane components are reported in Table 3. In the ^{1}H NMR spectrum (400 MHz) of the [2]catenane (*RS*)-**21**·4PF$_6$ above room temperature, the dynamic processes 1 and 2 are occurring at a fast rate on the NMR timescale. Two different sets of methylene proton resonances are observed (Figure 8). The first set, those linking the bipyridinium units to the binaphthyl spacer, appear as an AX system, δ 6.12 and 6.29,

Table 3. Chemical shift data [δ values (Δδ values)] [a] obtained from the 400 MHz ^{1}H NMR spectra recorded for the [2]catenanes (*R*)-**21**·4PF$_6$, (*RR*)-**29**·4PF$_6$ and the cyclophanes (*R*)-**23**·4PF$_6$, (*RR*)-**26**·4PF$_6$ bearing binaphthyl spacers in CD_3COCD_3 solutions at room temperature.

Compound	Charged component			
	α-CH	β-CH	C_6H_4 [b]	CH_2N^+
(*R*)-**23**·4PF$_6$	9.43/9.40	8.64/8.62	7.95	6.42(d)/6.21(d)/6.15(s)
(*R*)-**21**·4PF$_6$ [c]	9.35/9.18	8.19/8.12	8.06	6.29(d)/6.12(d)/6.10(s)
	(−0.09/−0.22)	(−0.35/−0.40)	(+0.11)	(−0.13/−0.09/−0.05)
(*RR*)-**26**·4PF$_6$	9.48	8.68		6.45(d)/6.20(d)
(*RR*)-**29**·4PF$_6$	9.05/8.95	7.72/7.15		6.20(d)/5.98(d)
	(−0.43/−0.53)	(−0.96/−1.53)		(−0.25/−0.22)

[a] The Δδ values indicated in parentheses under the respective δ values relate to the changes in chemical shift exhibited by the probe protons upon catenane formation. A negative value indicates a movement of the resonance to high field. [b] The C_6H_4 refers to the *p*-xylyl components of charged components. [c] Spectra recorded at 320 K.

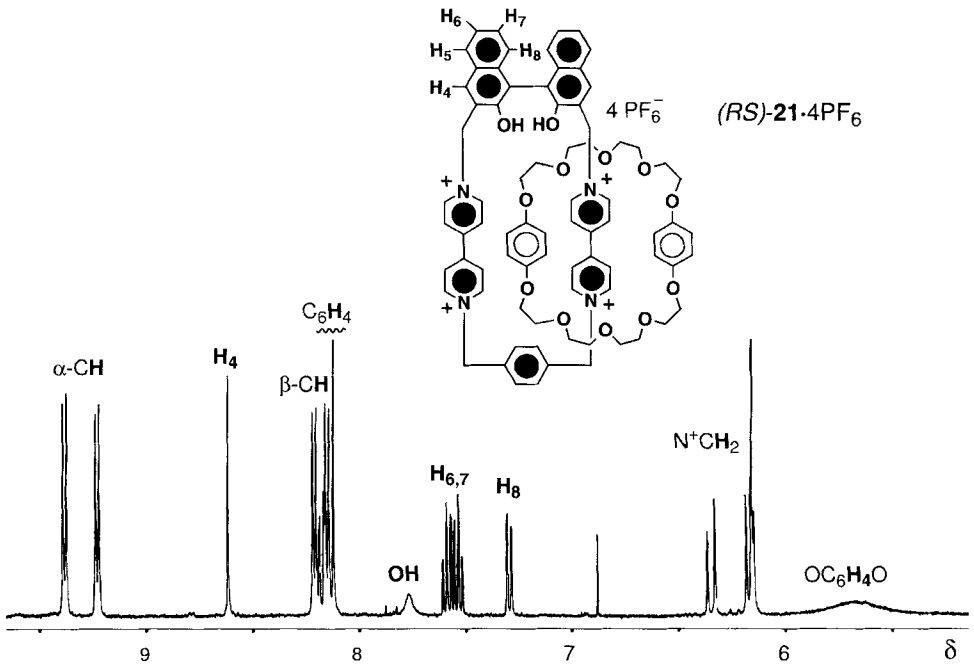

Figure 8. The ^{1}H NMR spectrum of the [2]catenane (*RS*)-**21**·4PF$_6$ at 30 °C (400 MHz) in CD_3COCD_3/CD_3NO_2 (4/1 v/v).

as a result of the diastereotopicity of the geminal pairs. The other set, remote from the chiral spacer, is less sensitive to the chiral environment and resonates as an apparent singlet at δ 6.10. A single broad resonance is observed for the protons of hydroquinone rings of the crown ether at δ 5.68. The dynamic processes taking place within the [2]catenane (*RS*)-**21**·4PF$_6$ were investigated by means of variable temperature methods (400 MHz). However, unambiguous delineation of the exchange processes occurring in the system was not achieved at moderate field strength. When a solution of (*RS*)-**21**·4PF$_6$ in CD_3COCD_3/CD_3NO_2 is cooled down to 273 K, process 1 (Scheme 10) becomes slow on the NMR timescale (400 MHz), and "inside" and "alongside" hydroquinone environments become distinguishable (δ = 6.30 and 4.90), although the "inside" hydroquinone ring proton resonance remains broad, indicative of the simultaneous slowing of other exchange processes. At temperatures below 250 K, we observed an increasing degree of broadening and complexity throughout the entire spectrum. Inspection of CPK space-filling molecular models suggests that it

0947-6539/97/0303-0472 $ 15.00+.25/0 Chem. Eur. J. 1997, 3, No. 3

is not possible for the crown ether to slip over the bulky binaphthyl residue (vide infra). We therefore assume that process 2 will be occurring, but in a restricted sense, that is, that the tetracationic cyclophane is free to swing around the "inside" hydroquinone ring of the **BPP34C10** component but it cannot circumrotate through the cavity. Such a process, when fast on the NMR timescale, would result in an averaging of the signals observable for related chemical environments of the tetracationic cyclophane component. Other, more subtle, exchange processes such as the slowing of the rocking motion of the hydroquinone rings of the **BPP34C10** component within the cavity of the tetracationic cyclophane component may also be contributing to broadening of the spectra.[31]

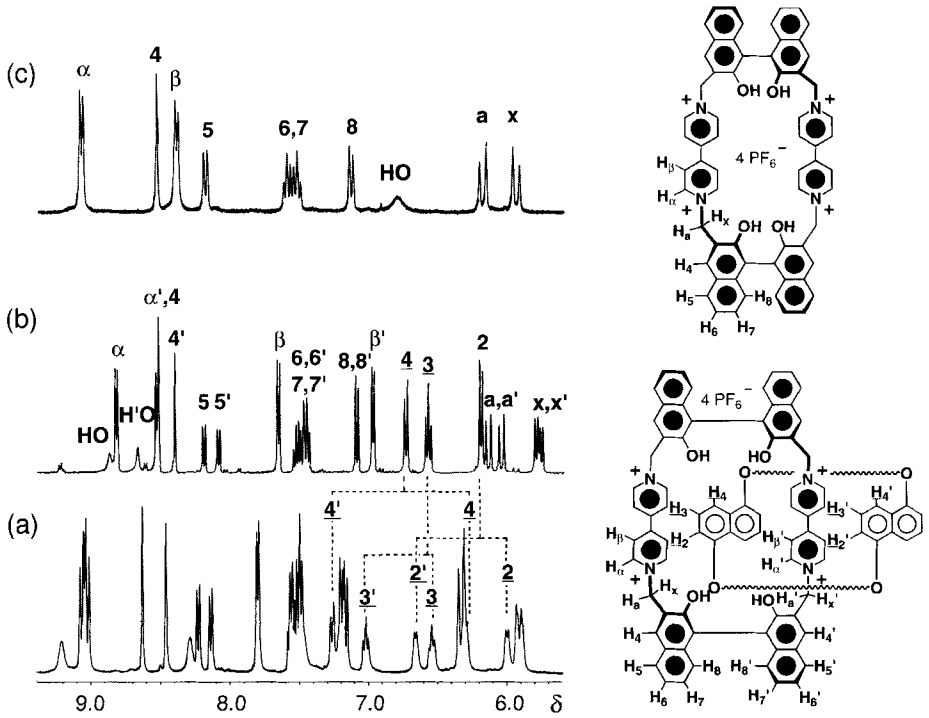

Figure 9. Comparison of the ^{1}H NMR spectra recorded for a) the [2]catenane (*RR*)-**29**·4PF$_6$ (400 MHz, 225 K, CD_3COCD_3), b) the [2]catenane (*RR*)-**29**·4PF$_6$ (400 MHz, 340 K, CD_3COCD_3) and c) the cyclophane (*RR*)-**26**·4PF$_6$ (300 MHz, 300 K, CD_3COCD_3). The polyether chains of the crown ether components are omitted for clarity.

The variable-temperature ^{1}H NMR spectra of the optically active [2]catenane (*RR*)-**29**·4PF$_6$, incorporating two bulky (*R*)-binaphthol units in its π-electron-deficient component, reveal a highly hindered system in which the neutral component is free to circumrotate through the charged component, but the passage of the tetracationic cyclophane component through the **1,5DN38C10** component is restricted. When a solution of (*RR*)-**29**·4PF$_6$ in CD_3COCD_3 is cooled to 225 K (Figure 9a), unique "inside" and "alongside" environments are distinguished for all of the aromatic protons of both the charged and neutral components—with the exception of the protons *peri* to the binaphthyl central aryl–aryl bonds—since both dynamic processes are slow on the ^{1}H NMR timescale (400 MHz) at this temperature. Upon warming the solution to 273 K, the resonances attributable to 1,5-dioxynaphthalene units coalesce as process 1 becomes fast on the ^{1}H NMR timescale ($\Delta G^{\neq}$ = 12.5 kcal mol^{-1} in Table 2). Further heating of a solution of the catenane in CD_3SOCD_3 does not, however, lead to the averaging of the resonances of the tetracationic cyclophane component (Figure 9b): "inside" and "alongside" environments are distinct even at 393 K at 270 MHz. This observation sets a lower limit on the free energy of activation for process 2 in this catenane of > 20 kcal mol^{-1}. The appearance of the spectra obtained for the catenane (*RR*)-**29**·4PF$_6$ can be contrasted with the spectrum of the corresponding, optically pure, tetracationic cyclophane (*RR*)-**26**·4PF$_6$ (Figure 9c). This free tetracationic cyclophane possesses D_2 symmetry and hence only one set of resonances is observed for each aromatic environment, as expected on the basis of its symmetry properties.

Association Constants: In the knowledge that $\mathbf{1}^{4+}$ forms strong 1:1 complexes with biologically important compounds,[13] the ability of the axially chiral receptors (*R*)-$\mathbf{23}^{4+}$ and (*RR*)-$\mathbf{26}^{4+}$ to exhibit enantiomeric differentiation toward amino acid carrying π-electron-rich aromatic rings was investigated. Although inspection of molecular models shows that (*R*)-$\mathbf{23}^{4+}$ and (*RR*)-$\mathbf{26}^{4+}$ have slightly enlarged and distorted cavities compared with $\mathbf{1}^{4+}$, both chiral tetracationic cyclophanes form strong 1:1 complexes with **BHEEB**: for (*R*)-**23**·4PF$_6$ and (*RR*)-**26**·4PF$_6$ in MeCN at 25 °C, the K_a values are 810 and 2510 M^{-1}, respectively, as determined by UV/vis titration. The association constant for the 1:1 complex formed between (*RR*)-**26**·4PF$_6$ and the 1,5-dioxynaphthalene-containing aromatic compound **BHEEN** is somewhat lower (330 M^{-1}), again as determined by UV/vis titration in MeCN at 25 °C.

The symmetry elements present in (*R*)-**23**·4PF$_6$ and (*RR*)-**26**·4PF$_6$ mean that, in both cases, the faces of the receptors are homotopic and thus, irrespective of which face binds the substrate, only one 1:1 complex can be formed by either (*R*)-**23**·4PF$_6$ or (*RR*)-**26**·4PF$_6$. Association constants, determined by UV/vis titration, and derived free energies of complexation for the 1:1 complexes formed between either (*R*)-**23**·4X (X = PF$_6$ or Cl)[32] or (*RR*)-**26**·4PF$_6$ and the L- and D-enantiomers of phenylalanine (Phe), tyrosine (Tyr), and tryptophan (Trp) (in the free, methyl esterified, and *N*-acetylated forms) in H_2O and organic solvents are listed in Table 4. Comparison of the K_a values between (*R*)-**23**·4Cl and L-Trp and D-Trp in H_2O (entries 1 and 2) indicate a modest amount of enantioselectivity in favor of D-Trp, which was reduced drastically when the corresponding L- and D-methyl ester hydrochloride salts were investigated (entries 3 and 4), suggesting that the carboxylic acid function in these amino acids might be playing a role in binding and enantioselection. When the amino groups on L-Trp and D-Trp were *N*-acetylated, the association constants in MeCN/DMF (90:10) were considerably increased and the enantioselectivity is larger and this time favors the L- over the D-enantiomer (entries 5 and 6). Interestingly, the enantiomeric differentiation

Table 4. Binding constants (K_a) and free energies of complexation ($-\Delta G^\circ$) for the 1:1 complexes formed between cyclophanes (*R*)-**23**·X (X = PF_6 or Cl) and (*RR*)-**26**·4PF_6 and π-electron-rich amino acids [a].

Entry	Substrate	Solvent	K_a (M^{-1})		K_a(L)/K_a(D)		$-\Delta G^\circ$ (kcal mol^{-1})		$\Delta\Delta G^\circ$ (kcal mol^{-1}) [b]	
			(*R*)-**23**	(*RR*)-**26**	(*R*)-**23**	(*RR*)-**26**	(*R*)-**23**	(*RR*)-**26**	(*R*)-**23**	(*RR*)-**26**
1	L-Trp	H_2O [c]	2470	ND [d]			4.63			
2	D-Trp	H_2O [c]	5860	ND [d]	0.42		5.14		−0.51	
3	L-Trp OMe·HCl	H_2O [c]	753	ND [d]			3.92			
4	D-Trp OMe·HCl	H_2O [c]	803	ND [d]	0.94		3.96		−0.04	
5	*N*-Ac-L-Trp	A [e]	20700	4280			5.89	4.95		
6	*N*-Ac-D-Trp	A [e]	2670	1080	7.75	3.96	4.67	4.14	1.22	0.81
7	*N*-Ac-L-Tyr	B [e]	10060	2340			5.45	4.60		
8	*N*-Ac-D-Tyr	B [e]	2125	1047	4.73	2.23	4.53	4.12	0.92	0.48
9	*N*-Ac-L-Phe	A [e]	1220	219			4.21	3.19		
10	*N*-Ac-D-Phe	A [e]	2260	137	0.54	1.60	4.57	2.91	−0.36	0.28

[a] All binding constants were determined by UV/Vis titration at 25 °C. [b] $\Delta\Delta G^\circ = \Delta G^\circ$(L)·$\Delta G^\circ$(D). [c] In H_2O as a solvent, (*R*)-**23**·4Cl was used. [d] Not determined. [e] Solvent mixture A: MeCN 90%, DMF 10%; solvent mixture B: MeCN 90%, DMSO 10%.

achieved by the cyclophane (*R*)-**23**·4PF_6 [K_a(L)/K_a(D) = 7.75] is higher than that obtained in organic solvents for (*RR*)-**26**·4PF_6 [K_a(L)/K_a(D) = 4.73]. The association constants for the 1:1 complexes formed between the cyclophane (*R*)-**23**·4PF_6 and the *N*-acetyltryptophan substrates are also higher than the ones obtained for the 1:1 complexes formed between the cyclophane (*RR*)-**26**·4PF_6 and the same *N*-acetyltryptophan substrates. The presence of an additional stabilizing T-type edge-to-face interaction[33] between the NH proton in the indole ring of the amino acid and the *p*-xylyl spacer present in (*R*)-**23**·4PF_6 might offer a possible explanation. This hypothesis is supported also by ^{1}H NMR chemical shift data for 1:1 mixtures of (*R*)-**23**·4PF_6 with *N*-acetyl-D-tryptophan (Figure 10c) and *N*-acetyl-L-tryptophan (Figure 10d): when compared with the spectra of the free cyclophane (Figure 10b), an upfield shift of the *p*-xylyl resonances of the cyclophane (0.13 ppm in the case of the D-enantiomer and 0.14 ppm in the case of the L-enantiomer) is observed. A downfield shift upon complexation ($\Delta\delta \approx 0.18$ and 0.30 ppm in each enantiomer) of the β proton resonances of the bipyridinium units of the cyclophane is also observed in agreement with other examples of inclusion complexes between π-electron-deficent bipyridinium-based cyclophanes and π-electron-rich guests.[34] Selected examples of UV/vis titrations are shown in Figure 11. The curves, obtained by adding increasing amounts of the *N*-acetyl amino acid guest to a solution of fixed concentration of the host (*R*)-**23**·4PF_6, show a decrease of the absorbance of the cyclophane (in the region 350–400 nm) with the formation of the 1:1 inclusion complex, and a developing, weak charge transfer band (450–500 nm) for the complex being formed. The charge transfer band is immediately evident in the case of *N*-acetyl-L-tryptophan (Figure 11a), whereas it is less evident in the case of *N*-acetyl-L-tyrosine and *N*-acetyl-L-phenylalanine (Figure 11b and 11c, respectively). Isosbestic points[35] were present in the curves from the titrations, strongly suggesting, in all cases, the presence of exclusively *one* 1:1 complex in solution. In both cyclophanes, the enantioselectivities decrease on going from *N*-acetyltryptophan to *N*-acetyltyrosine[36] (entries 7 and 8 in Table 4) and to the less π-electron-rich *N*-acetylphenylalanine (entries 9 and 10). All these data suggest to us a model in which the more π-electron-rich the guest is (primary mode of binding), the more the secondary stereoelectronic interactions of the functional groups of the guest with the bulky optically active binaphthol spacer(s) of the cyclophane(s) are effective in recognition terms.

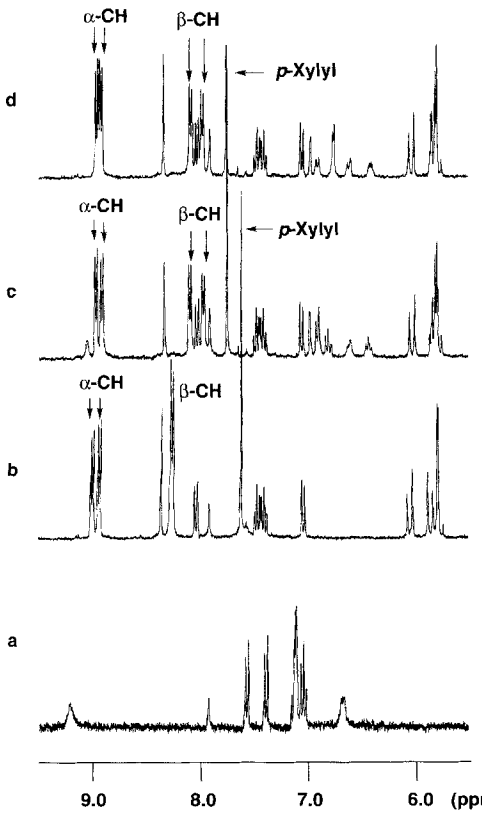

Figure 10. ^{1}H NMR spectra of 2 mM solutions in CD_3CN 90%/[D_7]DMF 10% of: a) *N*-acetyltryptophan; b) (*R*)-**23**·4PF_6; c) *N*-acetyl-D-tryptophan and (*R*)-**23**·4PF_6 (1:1); d) *N*-acetyl-L-tryptophan and (*R*)-**23**·4PF_6 (1:1).

Molecular Modeling: Molecular modeling was used in an attempt to predict the modes of interaction for the complexes formed between a) tryptophan and b) *N*-acetyltryptophan and the chiral tetracationic cyclophane (*R*)-**23**·4PF_6. Coordinates for (*R*)-**23**·4PF_6 were taken from the X-ray crystal structure of the correct enantiomer of (*RS*)-**21**·4PF_6, and those of the guest species were generated by the program Macromodel.[37] To be sure of sampling an adequate ensemble of the conformations available to complexes of this type, three different techniques—stochastic dynamics (SD), mixed-mode Monte Carlo/stochastic dynamics (MC/SD) and Monte Carlo conformational search

0947-6539/97/0303-0474 $ 15.00+.25/0 Chem. Eur. J. 1997, 3, No. 3

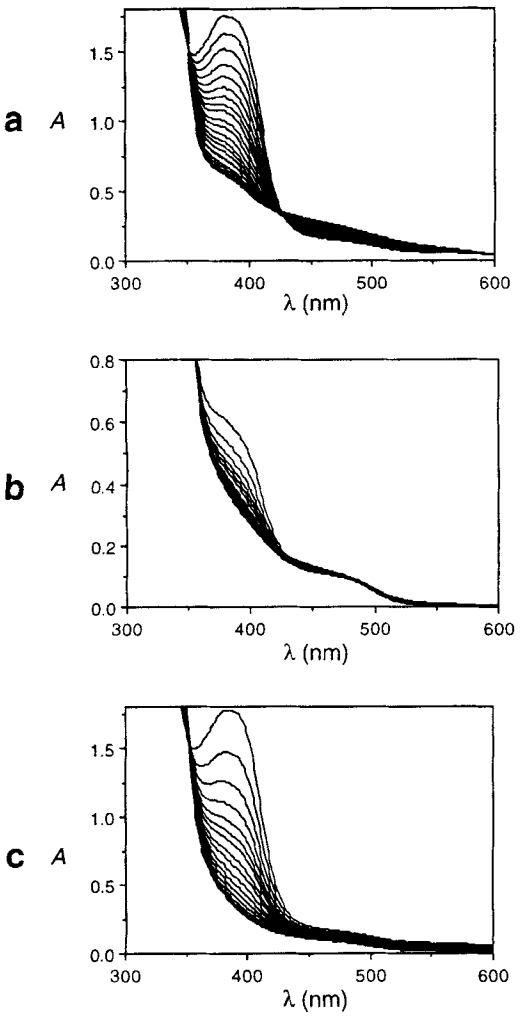

Figure 11. Curves obtained from the UV/Vis titrations of (*R*)-**23**·4PF$_6$ with: a) *N*-acetyl-L-tryptophan; b) *N*-acetyl-L-tyrosine; c) *N*-acetyl-L-phenylalanine.

techniques (MC)—with two separate solvation models and three different force fields were utilized. In our hands, the Monte Carlo technique proved to be the most versatile when used in conjunction with the Amber* forcefield, as both the MM2 and OPLS forcefields are not particularly well parameterized for these types of systems; each has low-quality parameters for the tetracationic cyclophane moiety. The computational study predicted that the π-electron-rich aromatic rings would be positioned almost centrally within the tetracationic cyclophane component and, as such, sandwiched between the π-electron-deficient bipyridinium rings. In addition, there appear to be CH–π-type interactions[38] between the indole N–H hydrogen atom and the *p*-xylyl residue (H–centroid distances between 2.3–2.4 Å) in the cyclophane, consistent with many of the solid-state structures for inclusion complexes of this type.[39] Analyses of the predicted structures for D- and L-tryptophan suggest that it is the carbonyl oxygen in the carboxylic acid function of the amino acid that participates in a hydrogen-bonding interaction with a hydroxyl function of the binaphthol unit. Similarly, examination of the *N*-acetylated system suggests that, in all the low-energy conformations, it is the carbonyl function of the acetyl unit that interacts, through hydrogen bonds, with the proximal hydroxyl function of the binaphthol unit (Figure 12).

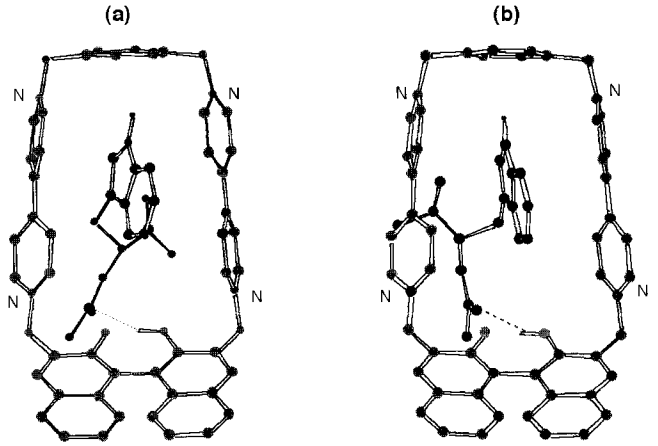

Figure 12. Computer-generated structures for the inclusion complexes formed between (*R*)-**23**·4PF$_6$ and a) *N*-acetyl-D-tryptophan and b) *N*-acetyl-L-tryptophan.

Furthermore, the data suggests that the *N*-acetylation of the amino acid results in the formation of a guest species that possesses a higher degree of stereoelectronic complementarity with the chiral cavity of the tetracationic cyclophane. This observation is in good agreement with the experimental results, as the *N*-acetylated systems show significant increases in binding energies when compared to the free amino acids. An examination of the relative energies of the 1:1 complexes formed between (*R*)-**23**·4PF$_6$ and the D- and L-enantiomers of tryptophan and *N*-acetyltryptophan, however, revealed little significant energetic preference for one enantiomer over the other. Submission of the structures representing the global minima of the complexes to AM1 and PM3 semiempirical analyses[40] also provided little information regarding the observed enantioselectivity, suggesting that the chiral discrimination is a consequence of subtle noncovalent interactive forces that—at least in our hands—cannot be reproduced with the aforementioned computational techniques.

Conclusions

The research described in this paper has shown how apparently complex molecular compounds, in the shape of [2]catenanes, can be constructed by means of self-assembly, and how π-electron-rich templates can be employed to assist in the building of π-electron-deficient cyclophanes. The introduction of bitolyl spacers into the skeleton of **1**$^{4+}$ has proved the viability of a possible route toward the self-assembly of catenanes and receptors that are axially chiral. The optically active *[2]catenanes* (*R*)-**21**·4PF$_6$ and (*RR*)-**29**·4PF$_6$ have been self-assembled in good yields and the optically active π-electron-deficient tetracationic cyclophanes (*R*)-**23**·4PF$_6$ and (*RR*)-**26**·4PF$_6$ have been shown to differentiate enantioselectively between amino acids bearing π-electron-rich aromatic residues as a result of subtle differences in the supramolecular interactions (π–π stacking and hydrogen bonding), which are also responsible for the self-assembly of the [2]catenanes. The information gained from studying both the solid- and solution-state structures of the [2]catenanes described in this paper shows that the molecular recognition ability responsible for their self-assembly persists

thereafter. The functionalization of the hydroxyl group on the tetracationic components of the cyclophanes and catenanes has been achieved in good yields, showing how chemistry can be performed on these charged organic salts.[41] We believe that we have developed an efficient way of introducing chirality into the tetracationic cyclophane components of our catenanes. We are now poised to introduce chirality into the crown ether components of these same catenanes and observe the degree to which self-assembly processes exhibit stereoselectivity when mechanical bonds are put in place between chiral components.

Experimental Section

General Methods: Chemicals were purchased from Aldrich and used as received. Solvents were dried [PhMe, CH_2Cl_2, CH_2Cl_2 (with CaH_2), MeCN (P_2O_5) and THF (Na/Ph_2CO)] according to procedures described in the literature.[42] The compounds **BHEEB**,[12b] **BPP34C10**,[12b] **BHEEN**,[28] **1,5DN38C10**,[26] 2,2′-bis(bromomethyl)-1,1′-binaphthyl ((*RS*)-**5**),[43] 1,1′-[1,4-phenylenebis(methylene)]bis(4,4′-bipyridinium) bis(hexafluorophosphate) (**7**·$2PF_6$),[12b] and *N*-acetyl-D-tyrosine[36] were prepared according to literature procedures. L-Leucine methyl ester was prepared by stirring an aqueous solution of the corresponding commercially available hydrochloride salt with a saturated solution of $NaHCO_3$ and extracting the product with CH_2Cl_2. The reactions requiring ultrahigh pressure were carried out in a Teflon vessel with a custom-built ultrahigh pressure press, manufactured by PSIKA Pressure Systems Limited of Glossop (UK). Thin-layer chromatography (TLC) was carried out on aluminum sheets precoated with silica gel 60 F (Merck 5554). The plates were inspected by UV light and developed with iodine vapor. Column chromatography was carried out with silica gel 60 F (Merck 9385, 230–400 mesh). Melting points were determined on an Electrothermal 9200 apparatus and are not corrected. UV/Vis spectra were recorded on a Perkin–Elmer Lambda 2 with HPLC-quality solvents. ^1H NMR spectra were recorded either on a Bruker AC 300 (300 MHz) spectrometer or on a Bruker AMX 400 (400 MHz) spectrometer with either the solvent or TMS as internal standard. ^{13}C NMR spectra were recorded on either a Bruker AC 300 (75.5 MHz) or a Bruker AMX 400 (100.6 MHz) spectrometer with either the solvent or TMS as internal standards. All chemical shifts are quoted on the δ scale. Low-resolution mass spectra were performed with a Kratos Profile spectrometer, operating in electron-impact (EIMS) mode. Fast atom bombardment mass spectra (FAB MS) were recorded on a Kratos MS 80 spectrometer operating at 8 keV with a xenon primary atom beam. The matrix used was 3-nitrobenzyl alcohol (NOBA). Microanalyses were performed by the University of Birmingham Microanalytical Service and by the University of North London Microanalytical Service.

Compound (*RS*)-6·2PF$_6$: A solution of (*RS*)-**5** (0.2 g, 0.45 mmol) was added over a period of 6 h to a solution of 4,4′-bipyridine (0.5 g, 3.15 mmol) in dry MeCN (10 mL) under reflux under nitrogen. The solution was then heated under reflux overnight. The solvent was removed in vacuo and the crude reaction mixture purified by column chromatography (SiO_2, eluent MeOH/2 M aq. $NH_4Cl/MeNO_2$, 7:2:1). The solvents were removed in vacuo, the residue dissolved in H_2O, and a saturated aqueous solution of NH_4PF_6 added until no further precipitation occurred. The precipitate was filtered and dried to afford (*RS*)-**6**·$2PF_6$ as light blue crystals (0.2 g, 40%). M.p. 150–152 °C (decomp.); ^1H NMR (300 MHz, CD_3COCD_3, 25 °C, TMS): δ = 8.81 (d, 4H; pyridinium α-C*H*), 8.43 (d, 4H; pyridyl α-C*H*), 8.41 (d, 2H; binaphthyl *H*-3), 8.27 (d, 2H; binaphthyl *H*-4), 8.03 (d, 2H; binaphthyl *H*-5), 7.95 (d, 4H; pyridinium β-C*H*), 7.69 (d, 4H; pyridyl β-C*H*), 7.30 (m, 2H; binaphthyl *H*-6), 6.96 (m, 2H; binaphthyl *H*-7), 6.53 (d, 2H; binaphthyl *H*-8), 6.28 (d, 2H; NCH_2), 6.17 (d, 2H; NCH_2); ^{13}C NMR (75.5 MHz, CD_3COCD_3, 25 °C): δ = 154.3, 151.9, 145.7, 141.5, 135.9, 134.4, 133.1, 131.6, 131.1, 130.7, 129.4, 128.4, 128.3, 125.9, 125.9, 122.5, 64.6; MS (8 keV, FAB): *m/z* = 737 [*M* − PF_6]$^+$, 591 [*M* − 2PF_6]$^+$; HRMS (LSIMS) $C_{42}H_{32}N_4PF_6$: [*M* − PF_6]$^+$ calcd. 737.2269, found 737.2269.

3,3′-Bis(bromomethyl)biphenyl (10):[44] 3,3′-Dimethylbiphenyl (500 mg, 2.74 mmol), *N*-bromosuccinimide (1.074 g, 6.04 mmol), and benzoyl peroxide (20 mg) were suspended in CCl_4 (40 mL). The solution was heated under reflux for 3 h, after which time no more starting material was present as shown by TLC analysis (eluent: hexane/CH_2Cl_2 80/20). The resulting suspension was cooled to room temperature, the precipitated succinimide was filtered off, and the solvent was removed in vacuo to give **10** as a white solid, which was recrystallized from hexane (610 mg, 65%). M.p. 102–103 °C, ref. [44] m.p. 106–107 °C; ^1H NMR (300 MHz, $CDCl_3$, 25 °C, TMS): δ = 7.61 (brs, 2H; *H*-2), 7.53 (d, 2H; *H*-4), 7.47 (d, 2H; *H*-6), 7.40 (t, 2H; *H*-5), 4.58 (s, 4H; -CH_2-); ^{13}C NMR (75.5 MHz, $CDCl_3$, 25 °C): δ = 141.2, 138.4, 129.4, 128.2, 127.9, 127.3, 33.4; MS (70 eV, EI): *m/z* (%) = 340 (8) [*M*]$^+$, 260 (54) [*M* − Br]$^+$, 180 (56) [*M* − 2Br]$^+$.

[2]Catenane 14·4PF$_6$—Method A: **7**·$2PF_6$ (250 mg, 0.352 mmol), **BPP34C10** (470 mg, 0.882 mmol) and **10** (120 mg, 0.352 mmol) were dissolved in dry MeCN (50 mL). The solution turned red after 18 h, and a red precipitate began to form. Stirring was continued for 7 days at room temperature. The solvent was removed in vacuo to give a strongly colored material. Hot H_2O (30 mL) was added to the residue and the resulting suspension filtered. A solution of NH_4PF_6 in H_2O was added to the red solution. A red precipitate formed immediately. It was collected and crystallized from Me_2CO/H_2O, affording **14**·$4PF_6$ as a pure compound (136 mg). The strongly colored residue was purified by column chromatography (SiO_2, eluent MeOH/2 M aq. $NH_4Cl/MeNO_2$, 7:2:1) affording, after counterion exchange, another portion of **14**·$4PF_6$ (65 mg, total yield 33%). M.p. > 250 °C; ^1H NMR (400 MHz, CD_3COCD_3, 0 °C, TMS): δ = 9.34 and 9.13 (2 × d, 2 × 4H; bipyridinium α-C*H*), 8.15 and 8.10 (2 × d, 2 × 4H; bipyridinium β-C*H*), 8.02 (s, 4H; *p*-xylyl H), 7.89–7.83 (m, 4H; bitolyl H), 7.79–7.70 (m, 4H; bitolyl H), 6.23 (brs, 4H; "alongside" hydroquinone), 6.11 (s, 4H; NCH_2), 6.09 (s, 4H; NCH_2), 4.66 (brs, 4H; "inside" hydroquinone), 3.95–3.83 (m, 16H; -CH_2O-), 3.73–3.62 (m, 16H; -CH_2O-), 3.54–3.48 (m, 16H; -CH_2O-); ^{13}C NMR (75.5 MHz, CD_3COCD_3, 25 °C): δ = 153.8, 148.1, 147.7, 146.1, 146.0, 143.3, 137.4, 134.8, 131.5, 130.9, 130.5, 130.2, 129.1, 126.9, 126.3, 115.2, 71.3, 71.0, 70.6, 68.0, 65.5, 65.4; MS (8 keV, FAB): *m/z* = 1712 [*M*]$^+$, 1567 [*M* − PF_6]$^+$, 1422 [*M* − 2PF_6]$^+$, 1277 [*M* − 3PF_6]$^+$, 1031 [*M* − **BPP34C10** − PF_6]$^+$, 886 [*M* − **BPP34C10** − 2PF_6]$^+$, 741 [*M* − **BPP34C10** − 3PF_6]$^+$. $C_{70}H_{76}N_4O_{10}P_4F_{24}$ (1712.4): calcd C 49.05, H 4.47, N 3.27; found C 49.33, H 4.62, N 3.23. Single crystals, suitable for X-ray crystallography, were grown by vapor diffusion of *i*Pr_2O into a Me_2CO solution of the [2]catenane.

Method B: **11**·$2PF_6$ (40 mg, 0.051 mmol), **BPP34C10** (68 mg, 0.128 mmol), and 1,4-bis(bromomethyl)benzene **8** (16 mg, 0.061 mmol) were dissolved in dry MeCN (50 mL) and the solution stirred for 7 days at room temperature. The solvent was removed in vacuo to give a strongly colored material, which was purified by column chromatography (SiO_2, eluent MeOH/2 M aq. $NH_4Cl/MeNO_2$, 7:2:1) affording, after counterion exchange, **14**·$4PF_6$ (52 mg, 60%).

Compound 11·$2PF_6$: A solution of **10** (150 mg, 0.44 mmol) in dry MeCN (30 mL) was added dropwise to a refluxing solution of 4,4′-bipyridine (960 mg, 6.14 mmol) in dry MeCN (50 mL) over a period of 6 h under nitrogen. The solvent was removed in vacuo and the reaction mixture purified by column chromatography (SiO_2, eluent MeOH/2 M aq. $NH_4Cl/MeNO_2$, 7:2:1). Product-containing fractions were stripped of the solvent in vacuo, the residue was dissolved in H_2O, and a saturated solution of NH_4PF_6 in H_2O was added until no further precipitation occurred. The precipitate, **11**·$2PF_6$, was filtered and air-dried (160 mg, 47%). M.p. 160–162 °C (decomp.); ^1H NMR (300 MHz, CD_3COCD_3, 25 °C, TMS): δ = 9.39 (d, 4H; pyridinium α-C*H*), 8.87 (brs, 4H; pyridyl α-C*H*), 8.67 (d, 4H; pyridinium β-C*H*), 8.10 (s, 2H; bitolyl *H*2), 7.98 (d, 4H; pyridyl β-C*H*), 7.85 (d, 2H; bitolyl *H*4), 7.73 (d, 2H; bitolyl *H*6), 7.63 (t, 2H; bitolyl *H*5), 6.17 (s, 4H; NCH_2); ^{13}C NMR (75.5 MHz, CD_3COCD_3, 25 °C): δ = 155.2, 151.9, 146.1, 142.0, 142.0, 135.0, 131.0, 129.5, 129.3, 129.0, 127.1, 127.0, 65.0; MS (8 keV, FAB): *m/z* = 637 [*M* − PF_6]$^+$, 491 [*M* − 2PF_6]$^+$.

[2]Catenane 15·4PF$_6$—Method A: **11**·$2PF_6$ (56 mg, 0.072 mmol), **BPP34C10** (115 mg, 0.215 mmol), and **10** (29 mg, 0.086 mmol) were dissolved in dry MeCN (30 mL). The solution turned red after 2 days and a red solid began to precipitate. Stirring was continued for 10 days at room temperature. The solvent was removed in vacuo and the residue purified by column chromatography (SiO_2, eluent MeOH/2 M aq. $NH_4Cl/MeNO_2$, 7:2:1). The solvent from product-containing fractions was removed in vacuo, the residue was dissolved in H_2O, and a saturated solution of NH_4PF_6 in H_2O added until no further precipitation occurred. The red solid obtained was crystal-

0947-6539/97/0303-0476 $ 15.00+.25/0 Chem. Eur. J. 1997, 3, No. 3

lized once from Me_2CO/H_2O, affording **15**·4PF_6 as a pure compound (20 mg, 15%). M.p. >250 °C; ^{1}H NMR (300 MHz, CD_3COCD_3, 25 °C, TMS): δ = 9.16 (d, 8H; bipyridinium α-C*H*), 8.16 (d, 8H; bipyridinium β-C*H*), 7.93–7.85 (m, 12H, bitolyl *H*4, *H*2, *H*6), 7.75 (m, 4H, bitolyl *H*5), 6.13 (s, 8H; NCH_2), 5.84 (s, 8H, hydroquinone), 3.79–3.71 (m, 16H, $-CH_2O-$), 3.58–3.52 (m, 8H, $-CH_2O-$), 3.42–3.36 (m, 8H, $-CH_2O-$); ^{13}C NMR (75.5 MHz, CD_3COCD_3, 25 °C): δ = 152.8, 148.4, 146.3, 142.6, 134.3, 131.1, 129.9, 128.7, 126.8, 126.8, 115.5, 71.1, 71.0, 70.5, 68.3, 65.4; MS (8 keV, FAB): *m/z* = 1643 $[M - PF_6]^+$, 1498 $[M - 2PF_6]^+$, 1353 $[M - 3PF_6]^+$, 1107 $[M$ – **BPP34C10** $- PF_6]^+$, 962 $[M$ – **BPP34C10** $- 2PF_6]^+$, 817 $[M$ – **BPP34C10** $- 3PF_6]^+$; $C_{76}H_{80}N_4O_{10}P_4F_{24}$ (1788.4): calcd C 50.99, H 4.51, N 3.13; found C 50.41, H 4.40, N 3.18. Single crystals, suitable for X-ray crystallography, were grown by vapor diffusion of *i*Pr_2O into a MeCN solution of the [2]catenane.

Method B: **11**·2PF_6 (150 mg, 0.191 mmol), **BPP34C10** (410 mg, 0.764 mmol) and **10** (77 mg, 0.218 mmol) were dissolved in dry DMF (30 mL) and the solution was subjected to ultrahigh pressure (12 kbar) for 3 days. The solvent was removed in vacuo and the residue subjected to column chromatography (SiO_2, eluent MeOH/2 M aq. $NH_4Cl/MeNO_2$, 7:2:1). The solvent from product-containing fractions was removed in vacuo, the residue dissolved in H_2O and a saturated solution of NH_4PF_6 in H_2O added until no further precipitation occurred to afford **15**·4PF_6 (117 mg, 34%).

Cyclophane 16·4PF_6—Method A: **7**·2PF_6 (280 mg, 0.396 mmol), **10** (150 mg, 0.44 mmol), and **BHEEB** (757 mg, 2.64 mmol) were dissolved in dry MeCN (20 mL). The solution was stirred under nitrogen at room temperature for 14 days, and then the reaction mixture was poured into Et_2O (300 mL). The orange precipitate was filtered and dissolved in hot H_2O, and the orange solution was extracted continuously with $CHCl_3$ for 2 days until the organic layer became colorless. The product was subjected to column chromatography (SiO_2, eluent MeOH/2 M aq. $NH_4Cl/MeNO_2$, 7:2:1). The solvent in product-containing fractions was removed in vacuo, and the residue dissolved in H_2O. A saturated solution of NH_4PF_6 in H_2O was added until no further precipitation occurred. The precipitate, **16**·4PF_6, was filtered and air-dried (65 mg, 14%). M.p. >250 °C; ^{1}H NMR (300 MHz, CD_3COCD_3, 25 °C, TMS): δ = 9.52 and 9.39 (2 × d, 2 × 4H; bipyridinium α-C*H*), 8.64 and 8.59 (2 × d, 2 × 4H; bipyridinium β-C*H*), 7.89 (d, 2H; bitolyl *H*4), 7.78 (m, 6H; *p*-xylyl H and bitolyl *H*6), 7.61 (m, 4H; bitolyl *H*5, *H*2), 6.19 (s, 4H; NCH_2), 6.11 (s, 4H; NCH_2); ^{13}C NMR (75.5 MHz, CD_3CN, 25 °C): δ = 150.8, 150.6, 146.0, 142.8, 136.5, 134.7, 131.4, 131.1, 130.2, 130.0, 128.9, 128.3, 128.2, 128.1, 65.8, 65.5; MS (8 keV, FAB): *m/z* = 1031 $[M - PF_6]^+$, 886 $[M - 2PF_6]^+$, 741 $[M - 3PF_6]^+$; HRMS (LSIMS) $C_{42}H_{36}N_4P_3F_{18}$: $[M - PF_6]^+$ calcd. 1031.1865, found 1031.1882.

Method B: **7**·2PF_6 (280 mg, 0.396 mmol) and **10** (150 mg, 0.44 mmol) were dissolved in dry MeCN (20 mL) and the solution was stirred under nitrogen at room temperature for 14 days. The product was subjected to column chromatography (SiO_2, eluent MeOH/2 M aq. $NH_4Cl/MeNO_2$, 7:2:1). The solvent in product-containing fractions was removed in vacuo and the residue dissolved in H_2O. A saturated solution of NH_4PF_6 in H_2O was added until no further precipitation occurred. The precititate, **16**·4PF_6, was filtered and air-dried (29 mg, 6%).

Cyclophane 17·4PF_6—Method A: **11**·4PF_6 (160 mg, 0.204 mmol), **10** (85 mg, 0.245 mmol), and **BHEEB** (350 mg, 1.224 mmol) were dissolved in dry MeCN (50 mL). The solution was stirred under nitrogen at room temperature for 14 days. The reaction mixture was poured into Et_2O (300 mL); the orange precipitate was filtered and dissolved in hot H_2O, and the orange solution was extracted continuously with $CHCl_3$ for 2 days until the organic layer became colorless. The product was subjected to column chromatography (SiO_2, eluent MeOH/2 M aq. $NH_4Cl/MeNO_2$, 7:2:1). The solvent was stripped from the product-containing fractions in vacuo and the residue dissolved in H_2O. A saturated solution of NH_4PF_6 in H_2O was added until no further precipitation occurred. The precititate, **17**·4PF_6, was filtered and air-dried (51 mg, 20%). M.p. >250 °C; ^{1}H NMR (300 MHz, CD_3CN, 25 °C, TMS): δ = 8.95 (d, 8H; bipyridinium α-C*H*), 8.20 (d, 8H; bipyridinium β-C*H*), 7.77–7.62 (m, 16H; bitolyl *H*), 5.81 (s, 8H; NCH_2); ^{13}C NMR (75.5 MHz, CD_3CN, 25 °C): δ = 151.3, 146.3, 142.4, 134.5, 131.3, 130.6, 129.9, 129.1, 128.5, 65.8; MS (8 keV, FAB): *m/z* = 1107 $[M - PF_6]^+$, 962 $[M - 2PF_6]^+$, 817 $[M - 3PF_6]^+$; $C_{48}H_{40}N_4P_4F_{24}$ (1252.2): calcd C 46.00, H 3.22, N 4.40; found C 46.35, H 3.20, N 4.38.

Method B: **11**·4PF_6 (80 mg, 0.102 mmol) and **10** (43 mg, 0.123 mmol) were dissolved in dry MeCN (50 mL) and the solution was stirred under nitrogen at room temperature for 14 days. The product was subjected to column chromatography (SiO_2, eluent MeOH/2 M aq. $NH_4Cl/MeNO_2$, 7:2:1). The solvent from the product-containing fractions was removed in vacuo and the residue dissolved in H_2O. A saturated solution of NH_4PF_6 in H_2O was added until no further precipitation occurred. The precipitate, **11**·4PF_6, was filtered and air dried (21 mg, 16%).

2,2′-Dihydroxy-1,1′-binaphthyl-3,3′-dicarboxylic acid[24c] ((*RS*)-**18**): 3-Hydroxy-2-naphthalenecarboxylic acid (6 g, 31.9 mmol) and NaOH (1.2 g, 30 mmol) were dissolved in H_2O (110 mL) in a 500 mL three-neck round-bottomed flask. The solution was brought to reflux and a solution of $FeCl_3 \cdot 6H_2O$ (9 g, 34 mmol) in hot H_2O (50 mL) was added dropwise over a period of 30 min with vigorous mechanical stirring. A blue-green precipitate formed immediately. After the addition was completed, the mixture was refluxed for another hour. After cooling down to room temperature, the pH of the solution was adjusted to pH > 7 with a 2 N aqueous solution of NaOH. The suspension was filtered and concentrated. Concentrated HCl (10 M) was added to precipitate the product (pH < 2). The precipitate was filtered off, washed with H_2O and with a solution of $MeCO_2H$ in H_2O (80:20) to remove the unreacted starting material. The resulting yellow product (*RS*)-**18** was dried in vacuo (1 g, 33%). ^{1}H NMR (300 MHz, CD_3COCD_3, 25 °C, TMS): δ = 10.95 (s, 2H; COOH), 8.82 (s, 2H; *H*-4), 8.10 (m, 2H; *H*-5), 7.42 (m, 4H; *H*-6 and *H*-7), 7.16 (m, 2H; *H*-8); ^{13}C NMR (75.5 MHz, CD_3SOCD_3, 25 °C): δ = 172.2, 154.2, 136.6, 132.7, 129.9, 129.3, 126.8, 124.1, 123.8, 116.5, 114.8; MS (70 eV, EI): *m/z* (%) = 374 (100) $[M]^+$.

3,3′-Bis(hydroxymethyl)-2,2′-dihydroxy-1,1′-binaphthyl[24c] ((*RS*)-**19**): $LiAlH_4$ (300 mg, 8 mmol) was added carefully to a solution of (*RS*)-**18** (350 mg, 0.93 mmol) in dry THF (45 mL). The solution was then heated under reflux overnight under nitrogen. After cooling to room temperature, H_2O and then 10% aq. H_2SO_4 were added carefully. The reaction mixture was partitioned between Et_2O and H_2O. The organic layer was washed with H_2O and dried over $MgSO_4$, and the solvent was removed in vacuo. The residue was purified by column chromatography (SiO_2; eluent: AcOEt) thus affording (*RS*)-**19** (270 mg, 78%) of the desired product. M.p. 188–190 °C, ref.-[24c] m.p. 190–193 °C; ^{1}H NMR (300 MHz, CD_3SOCD_3, 25 °C, TMS): δ = 7.94 (s, 2H; *H*-4), 7.86 (d, 2H; *H*-5), 7.26 (t, 2H; *H*-6), 7.12 (t, 2H, *H*-7), 6.82 (d, 2H, *H*-8), 4.72 (dd, 4H; CH_2OH), 3.38 (brs, 2H; CH_2OH); ^{13}C NMR (75.5 MHz, CD_3COCD_3, 25 °C): δ = 153.0, 134.5, 131.6, 129.8, 128.6, 127.2, 126.5, 125.1, 123.8, 114.2, 61.9; MS (70 eV, EI): *m/z* (%) = 346 (53) $[M]^+$.

3,3′-Bis(bromomethyl)-2,2′-dihydroxy-1,1′-binaphthyl[24c] ((*RS*)-**20**): A 48% solution of HBr in $MeCO_2H$ (2 mL) was added dropwise to a stirred suspension of (*RS*)-**18** (120 mg, 0.32 mmol) in $MeCO_2H$ (20 mL) at room temperature. The reaction mixture was stirred for 1 h, then the solvent was removed in vacuo and the residue dissolved in Et_2O and washed with H_2O. The organic layer was dried over $MgSO_4$. The solvent was removed in vacuo and the crude (*RS*)-**20** was crystallized from hexane/PhMe (120 mg, 75%). M.p. 210–212 °C, ref. [24c] m.p. 215–216 °C; ^{1}H NMR (300 MHz, CD_3COCD_3, 25 °C, TMS): δ = 8.28 (s, 2H; O*H*), 8.14 (s, 2H; *H*-4), 7.92 (d, 2H; *H*-5), 7.31 (t, 2H; *H*-6), 7.25 (t, 2H; *H*-7), 6.98 (d, 2H; *H*-8), 4.95 (dd, 4H; $-CH_2Br$); ^{13}C NMR (75.5 MHz, CD_3COCD_3, 25 °C): δ = 153.2, 135.5, 132.4, 129.7, 129.0, 128.4, 127.9, 125.0, 124.4, 114.2, 30.5; MS (70 eV, EI): *m/z* (%) = 472 (42) $[M]^+$, 393 (87) $[M - Br]^+$, 311 (74) $[M - 2Br]^+$; $C_{22}H_{16}Br_2O_2$ (472.2): calcd C 55.90, H 3.40; found C 56.23, H 3.27.

Optical Resolution[24c] **of 2,2′-Dihydroxy-1,1′-binaphthyl-3,3′-dicarboxylic acid** ((*RS*)-**18**): A solution of optically pure L-leucine methyl ester (5.3 g, 36 mmol) {$[\alpha]_{589}^{26}$ = +19.4° (*c* = 0.21 in $CHCl_3$), reported[24c] $[\alpha]_{589}^{25}$ = +15.3° (neat)} in 50 mL of MeOH was added to a suspension of racemic (*RS*)-**18** (6.5 g, 17.3 mmol) in MeOH. The reddish-brown solution was heated in a water bath for 15 min and cooled to 25°C for 1 d and to 0 °C for 2 d. The salt that separated was filtered, washed with a small amount of MeOH, and dried to give 5.03 g of yellow crystals. The crystals were powdered in a mortar, and the powder was digested in hot MeOH (3 × 50 mL) with stirring for 1.5 h. The final powder (4 g) was dissolved in 50 mL of H_2O containing 0.6 g of NaOH. The resulting red solution was washed with Et_2O and acidified to pH 1 to give a yellow precipitate. The resulting yellow precipitate was washed with H_2O and dried to give (+)(*R*)-**18** (1.5 g, 23% yield based on racemate). The spectroscopic data for the optically active (+)(*R*)-**18** were

identical to those described for the racemic compound. $[\alpha]_{589}^{25} = +200°$ ($c = 0.015$ in THF), $[\alpha]_{589}^{25} = +175°$ ($c = 0.03$ in C_6H_5N) ref. [24c] $[\alpha]_{589}^{25} = +185°$ ($c = 1.08$ in C_6H_5N).

3,3′-Bis(hydroxymethyl)-2,2′-dihydroxy-1,1′-binaphthyl[24c] ((*R*)-**19**): $LiAlH_4$ (198 mg, 5.2 mmol) was added carefully to a solution of (*R*)-**18** (200 mg, 0.54 mmol) in dry THF (45 mL). The solution was then heated under reflux overnight under nitrogen. After cooling to room temperature, H_2O and then 10% aq. H_2SO_4 were added carefully. The workup was carried out as described above. The spectroscopic data for the optically active tetraol were identical to those described for the racemic compound. $[\alpha]_{546}^{25} = +76°$ ($c = 0.022$ in THF), ref. [24c] $[\alpha]_{546}^{25} = +78.7°$ ($c = 1.2$ in THF).

3,3′-Bis(bromomethyl)-2,2′-dihydroxy-1,1′-binaphthyl ((*R*)-**20**): A 48% solution of HBr in $MeCO_2H$ (4 mL) was added to a stirred suspension of (*R*)-**19** (240 mg, 0.5 mmol) in $MeCO_2H$ (20 mL). The reaction mixture was stirred for 1 h at room temperature. The workup was conducted as described above. The spectroscopic data for the optically active benzylic dibromide were identical to those described for the racemic compound. $[\alpha]_{589}^{25} = +87°$ ($c = 0.025$ in $CHCl_3$).

[2]Catenane (*RS*)-21·4PF$_6$: Compound (*RS*)-**20** (100 mg, 0.211 mmol), **7**·2PF$_6$ (135 mg, 0.191 mmol) and **BPP34C10** (255 mg, 0.478 mmol) were dissolved in dry MeCN (30 mL). After 4 h the solution became red and a precipitate began to form. The solution was stirred for 8 d. The solvent was then removed in vacuo and the residue subjected to column chromatography (SiO_2, eluent MeOH/2M aq. NH_4Cl/$MeNO_2$, 7:2:1). The solvent was stripped from the product-containing fractions in vacuo, and the residue dissolved in H_2O. A saturated solution of NH_4PF_6 in H_2O was added until no further precipitation occurred. The precipitate was dissolved in $MeNO_2$ and washed with H_2O. Removal of the solvent and crystallization from Me_2CO/H_2O afforded the [2]catenane (*RS*)-**21**·4PF$_6$ (190 mg, 54%). M.p. > 250 °C; ^{1}H NMR (400 MHz, CD_3COCD_3, 47 °C, TMS): $\delta = 9.35$ and 9.18 (2 × d, 2 × 4H; bipyridinium α-C*H*), 8.54 (s, 2H; binaphthyl H-4), 8.19 and 8.12 (2 × d, 2 × 4H; bipyridinium β-C*H*), 8.09 (d, 2H, binaphthyl H-5), 8.06 (s, 4H; *p*-xylyl *H*), 8.02 (brs, 2H; binaphthyl O*H*), 7.52 (t, 2H; binaphthyl H-6), 7.44 (t, 2H; binaphthyl H-7), 7.20 (d, 2H; binaphthyl H-8), 6.29 (d, 2H; NCH_2), 6.12 (d, 2H; NCH_2), 6.10 (s, 4H; NCH_2), 5.69 (brs, 8H; hydroquinone), 3.95–3.25 (bm, 32H, -CH_2O-); ^{13}C NMR (75.5 MHz, CD_3COCD_3, 25 °C): δ = 153.8, 153.7, 147.8, 147.3, 146.8, 137.6, 135.7, 135.0, 131.5, 129.9, 129.6, 129.2, 126.7, 125.5, 125.3, 124.8, 122.7, 116.1, 115.3, 113.6, 71.2, 71.0, 70.5, 70.3, 65.5, 63.4; MS (8 keV, FAB): *m/z* = 1699 [*M* − PF$_6$]$^+$, 1554 [*M* − 2PF$_6$]$^+$, 1410 [*M* − 3PF$_6$]$^+$, 1163 [*M* − **BPP34C10** − PF$_6$]$^+$, 1017 [*M* − **BPP34C10** − 2PF$_6$]$^+$, 872 [*M* − **BPP34C10** − 3PF$_6$]$^+$; $C_{78}H_{80}N_4O_{12}P_4F_{24}$·3$H_2O$ (1899.4): calcd C 49.32, H 4.56, N 2.95; found C 49.25, H 4.48, N 3.05. Single crystals suitable for X-ray crystallography were grown by liquid–liquid diffusion by layering *i*Pr$_2$O on top of a Me_2CO solution of the [2]catenane in an NMR tube.

[2]Catenane (*R*)-21·4PF$_6$: 3,3′-Bis(bromomethyl)-2,2′-dihydroxy-1,1′-binaphthyl (*R*)-**20** (35 mg, 0.1 mmol), **7**·2PF$_6$ (50 mg, 0.07 mmol), and **BPP34C10** (40 mg, 0.07 mmol) were dissolved in dry MeCN (30 mL). The reaction and the workup were carried out as described above. The spectroscopic data for the optically active [2]catenane were identical to those described for the racemic compound. $[\alpha]_{589}^{25} = +149°$, $[\alpha]_{570}^{25} = +159°$ ($c = 0.002$ in CH_3COCH_3). $C_{78}H_{80}N_4O_{12}P_4F_{24}$·3$H_2O$ (1899.4): calcd C 49.32, H 4.56, N 2.95; found: C 49.40, H 4.40, N 3.05.

Benzoylated [2]Catenane (*RS*)-22·4PF$_6$:(*RS*)-**21**·4PF$_6$ (30 mg, 0.016 mmol) was dissolved in dry MeCN (20 mL). An excess of benzoyl chloride and 2,6-dimethylpyridine was added and the solution stirred for 2 d at room temperature. The white precipitate was filtered off and the solvent removed in vacuo. The resulting red solid was subjected to column chromatography (SiO_2, eluent MeOH/2M aq. NH_4Cl/$MeNO_2$, 7:2:1) and counterion exchange to afford the dibenzoylated derivative in quantitative yield. ^{1}H NMR (300 MHz, CD_3COCD_3, 25 °C, TMS): $\delta = 9.28$ and 9.18 (2 × d, 2 × 4H; bipyridinium α-C*H*), 8.70 (s, 2H; binaphthyl H-4), 8.32 and 8.16 (2 × d, 2 × 4H; bipyridinium β-C*H*), 8.12 (s, 4H; *p*-xylyl *H*), 7.95 (d, 2H; binaphthyl H-5), 7.58 (t, 2H; binaphthyl H-6), 7.55 (m, 6H; binaphthyl H-7 and benzoyl *H*), 7.42 (d, 2H; binaphthyl H-8), 7.38 (t, 4H; benzoyl *H*), 7.26 (d, 2H; benzoyl *H*), 6.38 (d, 2H; NCH_2), 6.30 (d, 2H; NCH_2), 6.10 (brs, 4H; NCH_2), 5.40 (brs, 8H; hydroquinone), 4.00–3.30 (bm, 32H, -CH_2O-); ^{13}C NMR (75.5 MHz, CD_3COCD_3, 25 °C): δ = 164.0, 152.6, 148.8, 148.0, 147.0, 129.6 × 2, 127.1, 126.8, 126.6, 125.5 × 2, 115.4, 71.2, 71.0, 70.4, 68.2, 65.9, 64.5; MS (ESMS): *m/z* = 1909 [*M* − PF$_6$]$^+$, 1763 [*M* − 2PF$_6$]$^+$, 881 [*M* − 2PF$_6$]$^{2+}$; HRMS (LSIMS) $C_{92}H_{88}N_4O_{14}P_3F_{18}$: [*M* − PF$_6$]$^+$ calcd. 1907.5223, found 1907.5151.

Cyclophane (*R*)-23·4PF$_6$: **7**·2PF$_6$ (162 mg, 0.229 mmol), (*R*)-**20** (130 mg, 0.275 mmol), and **BHEEB** (261 mg, 0.912 mmol) were dissolved in dry MeCN (50 mL). The solution was stirred under nitrogen at room temperature for 14 d. The solvent from the reaction mixture was removed in vacuo. The orange precipitate was dissolved in 100 mL of MeOH/H_2O 1/1 and the orange solution was stirred with $CHCl_3$ for 2 h to dethread the template **bheeb**. The aqueous layer was separated, stripped of the solvent in vacuo and the product was subjected to column chromatography (SiO_2, eluent MeOH/2M aq. NH_4Cl/$MeNO_2$, 7:2:1). The solvent from the product-containing fractions was removed in vacuo and the residue dissolved in H_2O. A saturated solution of NH_4PF_6 in H_2O was added until no further precipitation occurred. The precititate (*R*)-**23**·4PF$_6$ was filtered and air dried (82 mg, 27%). $[\alpha]_{589}^{25} = +86°$, $[\alpha]_{578}^{25} = +91°$, $[\alpha]_{546}^{25} = +108°$ ($c = 0.009$ in CH_3COCH_3); ^{1}H NMR (300 MHz, CD_3CN, 25 °C, TMS): δ = 9.40 (m, 8H; bipyridinium α-C*H*), 8.62 (m, 8H; bipyridinium β-C*H*), 8.52 (s, 2H; binaphthyl H-4), 8.44 (s, 2H; binaphthyl O*H*), 8.05 (d, 2H; binaphthyl H-5), 7.95 (s, 4H; *p*-xylyl *H*), 7.47 (t, 2H; binaphthyl H-6), 7.38 (t, 2H; binaphthyl H-7), 7.10 (d, 2H; binaphthyl H-8), 6.42 (d, 2H; NCH_2), 6.21 (d, 2H; NCH_2), 6.15 (s, 4H; NCH_2); ^{13}C NMR (75.5 MHz, CD_3CN, 25 °C): δ = 153.7, 150.5, 150.3, 146.7, 146.1, 136.8, 135.8, 135.5, 131.4, 129.8, 129.7, 129.4, 128.2, 127.2, 125.5, 124.7, 121.9, 114.0, 65.8, 63.0; MS (8 keV, FAB): *m/z* = 1331 [*M* + Na]$^+$, 1163 [*M* + Na − PF$_6$]$^+$, 1018 [*M* − 2PF$_6$]$^+$, 873 [*M* − 3PF$_6$]$^+$; $C_{50}H_{40}N_4O_2P_4F_{24}$ (1308.2): calcd C 45.87, H 3.08, N 4.28; found C 45.95, H 3.53, N 4.26.

Benzoylated Cyclophane (*R*)-24·4PF$_6$: (*R*)-**23**·4PF$_6$ (59 mg, 0.045 mmol) was dissolved in dry MeCN (20 mL). An excess of benzoyl chloride and 2,6-dimethylpyridine was added and the solution stirred for 3 d at room temperature. The white precipitate was filtered off and the solvent removed in vacuo. The resulting red solid was subjected to column chromatography (SiO_2, eluent MeOH/2M aq. NH_4Cl/$MeNO_2$, 7:2:1), counterion exchange and recrystallization from Me_2CO/*i*Pr_2O to yield the dibenzoylated derivative (*R*)-**24**·4PF$_6$ as a yellow, glassy solid (39.1 mg, 57%). $[\alpha]_{589}^{25} = -7°$, $[\alpha]_{570}^{25} = -8°$, $[\alpha]_{546}^{25} = -11°$ ($c = 0.003$ in CH_3CN); ^{1}H NMR (300 MHz, CD_3COCD_3, 25 °C, TMS): δ = 9.33 and 9.06 (2 × d, 2 × 4H; bipyridinium α-C*H*), 8.59 (s, 2H; binaphthyl H-4), 8.40 and 8.32 (2 × d, 2 × 4H; bipyridinium β-C*H*), 8.07 (d, 2H; binaphthyl H-5), 7.87 (s, 4H; *p*-xylyl *H*), 7.64 (t, 2H; binaphthyl H-6), 7.54 (t, 2H; binaphthyl H-7), 7.42 (m, 4H; binaphthyl H-8 and benzoyl *H*), 7.20–7.09 (m, 8H; benzoyl *H*), 6.34 (d, 2H; NCH_2), 6.28 (d, 2H; NCH_2), 6.17 (s, 4H; NCH_2); ^{13}C NMR (75.5 MHz, CD_3COCD_3, 25 °C): δ = 164.6, 150.5, 149.5, 146.5, 146.1, 136.6, 135.5, 135.0, 134.5, 132.2, 131.4, 130.1, 127.6, 127.2, 126.5, 126.3, 124.7, 65.4, 62.7; MS (8 keV, FAB): *m/z* = 1371 [*M* − PF$_6$]$^+$, 1226 [*M* − 2PF$_6$]$^+$, 1081 [*M* − 3PF$_6$]$^+$; $C_{64}H_{48}N_4O_4P_4F_{24}$ (1516.2): calcd C 50.66, H 3.17, N 3.69; found C 50.71, H 2.91, N 3.40.

Compound (*R*)-25·2PF$_6$: A solution of (*R*)-**20** (120 mg, 0.25 mmol) in dry MeCN (30 mL) was added to a refluxing solution of 4,4′-bipyridine (2 g, 12.8 mmol) in dry MeCN (50 mL) under nitrogen over a period of 18 h. The solvent was removed in vacuo and the reaction mixture was purified by column chromatography (SiO_2, eluent MeOH/2M aq. NH_4Cl/$MeNO_2$, 7:2:1). The solvents from the product-containing fractions were removed in vacuo, the residue dissolved in H_2O, and a saturated solution of NH_4PF_6 in H_2O added until no further precipitation occurred. The precipitate was filtered and air-dried to yield (*R*)-**25**·2PF$_6$ as a yellow, glassy compound 143.9, 137.7, 136.6, 135.3, 134.4, 132.5, 132.1, 130.4, 130.3, 129.9, 129.7, (100 mg, 44%). M.p. > 250 °C; $[\alpha]_{589}^{25} = +15°$, $[\alpha]_{570}^{25} = +15°$, $[\alpha]_{546}^{25} = +17°$ ($c = 0.002$ in CH_3CN); ^{1}H NMR (300 MHz, CD_3COCD_3, 25 °C, TMS): δ = 9.45 (d, 4H; pyridinium α-C*H*), 8.84 (d, 4H; pyridyl α-C*H*), 8.67 (d, 4H; pyridinium β-C*H*), 8.48 (s, 2H; binaphthyl H-4), 8.02 (d, 2H; binaphthyl H-5), 7.95 (d, 4H; pyridyl β-C*H*), 7.43 (t, 2H; binaphthyl H-6), 7.31 (t, 2H; binaphthyl H-7), 7.00 (d, 2H; binaphthyl H-8), 6.35 (d, 2H; NCH_2), 6.28 (d, 2H; NCH_2); ^{13}C NMR (75.5 MHz, CD_3CN, 25 °C): δ = 153.4, 150.9, 146.3, 141.9, 135.7, 135.6, 134.4, 129.8, 129.4, 126.1, 126.0, 125.6, 124.7, 123.4, 122.9, 115.1, 62.0; MS (8 keV, FAB): *m/z* = 769 [*M* − PF$_6$]$^+$, 623 [*M* − 2PF$_6$]$^+$; $C_{42}H_{32}N_4O_2P_2F_{12}$ (914.2): calcd C 55.14, H 3.50, N 6.13; found C 55.13, H 3.51, N 5.87.

0947-6539/97/0303-0478 $ 15.00+.25/0 Chem. Eur. J. 1997, 3, No. 3

Cyclophane (*RR*)-26·4PF$_6$: A solution of (*R*)-**25**·2PF$_6$ (190 mg, 0.208 mmol), (*R*)-**20** (103 mg, 0.220 mmol), and **BHEEB** (314 mg, 11.0 mmol) were dissolved in dry MeCN (30 mL). The solution was stirred at room temperature for 14 d. The solvent was then removed in vacuo and the resulting solid was subjected to column chromatography (SiO_2, eluent MeOH/2M aq. NH_4Cl/$MeNO_2$, 7:2:1). The solvent from product-containing fractions was removed in vacuo and the residue dissolved in H_2O. A saturated solution of NH_4PF_6 in H_2O was added until no further precipitation occurred. The product was then dissolved in $MeNO_2$ and washed twice with H_2O to afford 170 mg of almost pure compound. Recrystallization from Me_2CO/iPr_2O yielded (*RR*)-**26**·4PF$_6$ as a yellow-brown, glassy solid (90 mg, 29%). $[\alpha]_{578}^{25} = +103°$, $[\alpha]_{546}^{25} = +120°$ ($c = 0.006$ in CH_3CN); ^{1}H NMR (300 MHz, CD_3CN, 25 °C, TMS): δ = 8.97 (d, 8H; bipyridinium α-C*H*), 8.43 (s, 4H; binaphthyl H-4), 8.29 (d, 8H; bipyridinium β-C*H*), 8.08 (d, 4H; binaphthyl H-5), 7.44 (t, 4H; binaphthyl H-6), 7.40 (t, 4H; binaphthyl H-7), 7.03 (d, 4H; binaphthyl H-8), 6.69 (brs, 4H; binaphthyl O*H*), 6.08 (d, 4H; NCH_2), 5.83, (d, 4H; NCH_2); ^{13}C NMR (75.5 MHz, CD_3COCD_3, 25 °C): δ = 153.5, 150.2, 146.6, 136.5, 136.5, 135.6, 129.6, 129.1, 127.2, 125.2, 125.0, 121.7, 114.2, 62.7; MS (8 keV, FAB): *m/z*: = 1371 $[M-PF_6]^+$, 1226 $[M-2PF_6]^+$, 1081 $[M-3PF_6]^+$; $C_{64}H_{48}N_4O_4P_4F_{24}$ (1516.2): calcd C 50.66, H 3.17, N 3.69; found C 50.69, H 3.03, N 3.55.

Benzoylated Cyclophane (*RR*)-27·4PF$_6$: (*RR*)-**26**·4PF$_6$ (28 mg, 0.018 mmol) was dissolved in dry MeCN (20 mL). An excess of benzoyl chloride and 2,6-dimethylpyridine was added and the solution stirred for 2 d at room temperature. The white precipitate was filtered off and the solvent removed in vacuo. The solid obtained was subjected to column chromatography (SiO_2, eluent MeOH/2M aq. NH_4Cl/$MeNO_2$, 7:2:1) and counterion exchange. The resulting solid was then dissolved in $MeNO_2$ and washed twice with H_2O and recrystallised from Me_2CO/iPr_2O to yield the dibenzoylated derivative (*RR*)-**27**·4PF$_6$ as a yellow, glassy solid (31 mg, 87%). $[\alpha]_{578}^{25} = +26°$ ($c = 0.002$ in CH_3CN); ^{1}H NMR (300 MHz, CD_3COCD_3, 25 °C, TMS): δ = 9.16 (d, 8H; bipyridinium α-C*H*), 8.67 (s, 4H; binaphthyl H-4), 8.49 (d, 8H; bipyridinium β-C*H*), 8.08 (d, 4H; binaphthyl H-5), 7.64 (t, 4H; binaphthyl H-6), 7.55 (t, 4H; binaphthyl H-7), 7.44–7.32 (m, 16H; benzoyl *H*), 7.20 (m, 8H; binaphthyl H-8 and benzoyl *H*), 6.37 (d, 4H; NCH_2), 6.29 (d, 4H; NCH_2); ^{13}C NMR (75.5 MHz, CD_3COCD_3, 25 °C): δ = 165.5, 150.2, 147.1, 146.5, 136.3, 135.4, 134.8, 132.6, 130.4, 129.7, 129.6, 128.3, 128.3, 127.5, 126.9, 126.7, 126.0, 125.0, 62.5; MS (8 keV, FAB): *m/z* = 1955 $[M+Na]^+$, 1788 $[M-PF_6]^+$, 1643 $[M-2PF_6]^+$, 1498 $[M-3PF_6]^+$; HRMS (LSIMS) $C_{92}H_{64}N_4O_8P_3F_{18}$: $[M-PF_6]^+$ calcd. 1787.3650, found 1787.3607.

"inside" binaphthyl H-5), 7.68 (d, 4H; "alongside" bipyridinium β-C*H*), 7.55–7.40 (m, 8H; binaphthyl H-5 and *H*-6), 7.10 (d, 4H; binaphthyl H-8), 6.96 (d, 4H; "inside" bipyridinium β-C*H*), 6.78 (d, 4H; naphthalene H-2,6), 6.60 (t, 4H; naphthalene H-3,7), 6.22 (d, 4H; naphthalene H-4,8), 6.20 (d, 2H; NCH_2), 6.10 (d, 2H; NCH_2), 5.81 (d, 4H; NCH_2), 4.10–3.60 (bm, 32H, -CH_2O-); ^{13}C NMR (75.5 MHz, CD_3COCD_3, 25 °C): δ = 153.5, 153.4, 153.1, 153.0, 147.4, 145.5, 144.9, 144.6, 136.6, 136.2, 136.0, 129.8, 129.7, 129.6, 129.2, 129.1, 126.8, 126.1, 125.9, 125.3, 125.2, 125.1, 125.0, 124.3, 124.2, 121.8, 121.7, 121.6, 121.5, 114.6, 106.4, 71.3, 71.2, 70.6, 70.5, 62.5, 62.4. MS (8 keV, FAB): *m/z* = 2171 $[M+NH_4]^+$, 2008 $[M-PF_6]^+$, 1862 $[M-2PF_6]^+$, 1718 $[M-3PF_6]^+$; $C_{100}H_{92}N_4O_{14}P_4F_{24}$ (2152.5): calcd C 55.76, H 4.28, N 2.60; found C 55.87, H 4.13, N 2.48.

X-Ray Crystallography: Table 5 provides a summary of the crystal data, data collection, and refinement parameters for the [2]catenanes **14**·4PF$_6$, **15**·4PF$_6$, and (*RS*)-**21**·4PF$_6$. Computations were carried out with the SHELXTL program system (version 5).[45]

Table 5. Crystal data, data collection and refinement parameters [a].

	14·4PF$_6$	**15**·4PF$_6$	(*RS*)-**21**·4PF$_6$
empirical formula [b]	$C_{70}H_{76}N_4O_{10}$·4PF$_6$	$C_{76}H_{80}N_4O_{10}$·4PF$_6$	$C_{78}H_{80}N_4O_{12}$·4PF$_6$
solvent	3Me_2CO	4MeCN·3/4H_2O	4.5Me_2CO
M_r	1887.5	1967.05	2106.69
color, habit	red block needles	orange needles	orange blocks
crystal size (mm)	0.50 × 0.37 × 0.30	0.71 × 0.24 × 0.17	0.50 × 0.27 × 0.15
temperature (K)	293	293	203
crystal system	monoclinic	triclinic	triclinic
space group	$P2_1/n$	$P\bar{1}$	$P\bar{1}$
a (Å)	10.961(1)	12.979(2)	13.523(1)
b (Å)	41.649(5)	13.532(2)	15.567(1)
c (Å)	20.557(2)	29.930(5)	24.789(2)
α (°)	90	88.52(2)	80.34(1)
β (°)	100.27(2)	85.78(1)	80.17(1)
γ (°)	90	64.62(2)	81.97(1)
V (Å^3)	9234(2)	4736(1)	5035.6(6)
Z	4	2	2
ρ_c (g cm^{-3})	1.358	1.379	1.389
radiation	$Cu_{K\alpha}$ [c]	$Cu_{K\alpha}$ [d]	$Cu_{K\alpha}$ [c]
μ (m^{-1})	1.701	1.678	1.647
F(000)	3904	2031	2184
2*θ* range (°)	4–110	6–110	4–120
independent reflns (R_{int})	11609 (0.05)	11817 (0.00)	14849 (0.04)
observed reflns [$\|F_o\| > 4\sigma(\|F_o\|)$]	6420	7010	10357
no. of parameters	1102	1245	1406
a,*b* in weighting scheme [e]	0.1967, 13.7575	0.1883, 8.1170	0.1713, 5.9011
extinction, χ	0.0002	0.0009	–
final R_1 (wR_2)	0.105 (0.291)	0.106 (0.295)	0.091 (0.255)
largest and mean Δ/σ	−0.391, 0.013	−0.206, 0.007	0.517, 0.073
data/parameter ratio	5.83	5.61	7.37
largest difference peak–hole (eÅ^{-3})	0.52, −0.37	0.96, −0.33	0.71, −0.46

[a] Details in common: graphite-monochromated radiation, ω-scans, refinement based on F^2. [b] Excluding solvent. [c] Siemens P4/RA diffractometer. [d] Siemens P4/PC diffractometer. [e] $w^{-1} = \sigma^2(F_o^2) + (aP)^2 + bP$.

[2]Catenane (*RR*)-**29**·4PF$_6$. 3,3′-Bis(bromomethyl)-2,2′-dihydroxy-1,1′-binaphthyl (*R*)-**20** (62 mg, 0.313 mmol), (*R*)-**25**·2PF$_6$ (100 mg, 0.109 mmol), and **1,5DN38C10** (173 mg, 0.273 mmol) were dissolved in dry MeCN (30 mL). A deep purple color and a purple precipitate appeared overnight. The solution was stirred at room temperature for 14 days. The solvent was removed in vacuo and the residue subjected to column chromatography (SiO_2, eluent MeOH/2M aq. NH_4Cl/$MeNO_2$, 7:2:1). The solvent from the product-containing fractions was removed in vacuo, and they were dissolved in H_2O. A saturated solution of NH_4PF_6 in H_2O was added until no further precipitation occurred. The precipitate was dissolved in $MeNO_2$ and washed with H_2O. Removal of the solvent and precipitation from Me_2CO/iPr_2O afforded the [2]catenane (*RR*)-**29**·4PF$_6$ (110 mg, 47%). M.p. > 250 °C; $[\alpha]_{589}^{25} = +356°$, $[\alpha]_{570}^{25} = +372°$ $[\alpha]_{546}^{25} = +379°$ ($c = 0.0002$ in CH_3CN); ^{1}H NMR (400 MHz, CD_3SOCD_3, 67 °C, TMS): δ = 8.91 (d, 2H; "alongside" binaphthyl O*H*), 8.87 (d, 4H; "alongside" bipyridinium α-C*H*), 8.71 (d, 2H; "inside" binaphthyl O*H*), 8.58 (d, 4H; "inside" bipyridinium α-C*H*), 8.51 (s, 2H; "alongside" binaphthyl H-4), 8.42 (s, 2H; "inside" binaphthyl H-4), 8.20 (d, 2H; "alongside" binaphthyl H-5), 8.10 (d, 2H;

In **14**·4PF$_6$, there is 60:40 disorder in two discrete parts of the polyether linkages and 65:35, 55:45, 55:45 and 70:30 disorder in the four PF_6^- anions. The three Me_2CO molecules are distributed over four sites with two full-occupancy molecules and two partial-occupancy (65:35) molecules. The major occupancy non-hydrogen atoms were refined anisotropically. The position of the hydrogen atoms were determined from Δ*F* maps and subsequently idealized and refined isotropically (riding model).

In **15**·4PF$_6$ two of the PF_6^- anions are disordered rotationally and resolved in two different positions with 50:50 occupancies. The [2]catenane is solvated by four MeCN molecules, one of which is separated into two different orientations (50:50 each) and by 0.75H_2O disordered in two positions with occupancies of 50:25, respectively. All non-hydrogen atoms, with the exception of the solvent H_2O molecules, were refined anisotropically. The six-membered rings in the structure were optimized. Hydrogen atoms were located in two idealized positions based on the geometry of their parent atoms and refined isotropically, applying the riding model.

In (*RS*)-**21**·4PF_6, two PF_6^- anions are disordered and separated into two different orientations, with equal occupancies (50:50). The polyether chain is disordered in four positions, three of them with a 50:50 occupancy and one with a 60:40 occupancy. Four and a half Me_2CO molecules were identified in the structure. All non-hydrogen atoms were refined anisotropically by means of distance constraints in the refinement of the polyether chain. The hydrogen atoms were located from different Fourier maps (ΔF) and subsequently refined isotropically with a riding-model approach and fixed isotropic thermal parameters.

Association Constants: During the spectrophotometric titrations, the change in the optical density of a solution of a complex was recorded while the relative concentration of the guest in the complex was increased with respect to the cyclophane. The stability constants (K_a) were determined in MeCN, 10% DMF/MeCN or 10% DMSO/MeCN solutions at 298 K. In each experiment, a solution of the cyclophane was made up in a volumetric flask and its optical density recorded in a cuvette (1 cm path length). A known quantity of the guest was added to the solution. The optical density of this solution of the 1:1 complex was recorded and the procedure repeated until no significant change in optical density was observed on addition of further guest. Molar ratios of the guest to the cyclophane used were in the range 0.1:1 to 30:1. The titration data were treated by a nonlinear curve-fitting program (Ultrafit, Biosoft, Cambridge, 1992), running on an Apple Macintosh personal computer.

Molecular Modeling: Molecular modeling was performed on a Silicon Graphics Indigo^2 workstation with the Macromodel GB/SA solvation model for either H_2O or $CHCl_3$ throughout. Stochastic dynamics (SD) were performed at temperatures of 300 and 600 K with 10 ps equilibration and 100 ps of data collection. Mixed-mode Monte Carlo/stochastic dynamics (MC/SD) simulations were performed at a bath temperature of 300 K with a 10 ps equilibration and 100 ps of data collection, allowing only the torsions associated with the amino acid unit to experience unrestrained motion. During both the SD and MC/SD runs, 100 structures were sampled from each run and minimized with the multiconformation minimization algorithm resident in Macromodel. Monte Carlo conformational searching was carried out over 1000 steps with the ring torsions associated with the tetracationic cyclophane constrained. Single-point semiempirical calculations were performed on a Silicon Graphics Power Indigo^2 with the semiempirical mode of Spartan.

Acknowledgments: This research was supported in the United Kingdom by the Engineering and Physical Sciences Reseach Council and by Glaxo Research and Development Limited, who provided postgraduate studentship support for D. P.

Received: August 7, 1996 [F434]

[1] a) J. S. Lindsey, *New J. Chem.* **1991**, *15*, 153–180; b) G. M. Whitesides, J. P. Mathias, C. T. Seto, *Science* **1991**, *254*, 1312–1319; c) D. Philp, J. F. Stoddart, *Synlett* **1991**, 445–448; d) D. B. Amabilino, J. F. Stoddart, *New Scientist* 19 Feb. **1994**, No. 1913, pp. 25–29; e) D. Philp, J. F. Stoddart, *Angew. Chem. Int. Ed. Engl.* **1996**, *35*, 1154–1195.

[2] W. Saenger, *Principles of Nucleic Acid Structure*, Springer, New York, **1986**.

[3] a) H. Fraenkel-Contrat, R. C. Williams, *Proc. Natl. Acad. Sci. U. S. A.* **1955**, *41*, 690–698; b) A. Klug, *Angew. Chem. Int. Ed. Engl.* **1983**, *22*, 565–582; c) K. Namba, G. Stubbrs, *Science* **1986**, *231*, 1401–1406.

[4] C. B. Anfisen, *Science* **1973**, *181*, 223–230.

[5] a) J.-M. Lehn, *Angew. Chem. Int. Ed. Engl.* **1990**, *29*, 1304–1319; b) R. Kramer, J.-M. Lehn, A. Marquis-Rigault, *Proc. Natl. Acad. Sci. U. S. A.* **1993**, *90*, 5394–5398; c) E. C. Constable, *Angew. Chem. Int. Ed. Engl.* **1991**, *30*, 1450–1451; d) E. C. Constable, A. J. Edwards, P. R. Raithby, J. V. Walker, *Angew. Chem. Int. Ed. Engl.* **1993**, *32*, 1465–1467.

[6] a) C. O. Dietrich-Buchecker, J.-P. Sauvage, *Chem. Rev.* **1987**, *87*, 795–810; b) J. C. Chambron, C. O. Dietrich-Buchecker, J.-P. Sauvage, *Top. Curr. Chem.* **1993**, *165*, 131–162; c) C. A. Hunter, *J. Am. Chem. Soc.* **1992**, *114*, 5303–5111; d) H. Adams, F. J. Carver, C. A. Hunter, *J. Chem. Soc. Chem. Commun.* **1995**, 809–810; e) F. Vögtle, S. Meier, R. Hoss, *Angew. Chem. Int. Ed. Engl.* **1992**, *31*, 1619–1622; f) M. Bauer, W. M. Müller, U. Müller, K. Rissanen, F. Vögtle, *Liebigs Ann.* **1995**, 649–656; g) A. G. Johnston, D. A. Leigh, R. J. Pritchard, M. D. Deegan, *Angew. Chem. Int. Ed. Engl.* **1995**, *34*, 1209–1212; h) A. G. Johnston, D. A. Leigh, L. Nehzat, J. P. Smart, M. D. Deegan, *ibid.* **1995**, *34*, 1212–1216.

[7] a) J. A. Zerkowski, C. T. Seto, D. A. Wierda, G. M. Whitesides, *J. Am. Chem. Soc.* **1990**, *112*, 9025–9026; b) J. A. Zerkowski, J. C. MacDonald, C. T. Seto, D. A. Wierda, G. M. Whitesides, *ibid.* **1994**, *116*, 2382–2391; c) J. P. Mathias, E. E. Simanek, G. M. Whitesides, *ibid.* **1994**, *116*, 4326–4340.

[8] a) H. Ringsdorf, B. Schlarb, J. Venzmer, *Angew. Chem. Int. Ed. Engl.* **1988**, *27*, 113–158; b) K. Fujita, S. Kimura, Y. Imanishi, E. Rump, H. Ringsdorf, *J. Am. Chem. Soc.* **1994**, *116*, 2185–2186; c) D. Lupo, H. Ringsdorf, A. Schuster, M. Seitz, *ibid.* **1994**, *116*, 10498–10506.

[9] D. B. Amabilino, J. F. Stoddart, *Chem. Rev.* **1995**, *95*, 2725–2828.

[10] a) M. C. Etter, *Acc. Chem. Res.* **1990**, *23*, 120–126; b) A. D. Hamilton, *J. Chem. Ed.* **1990**, *67*, 821–828; c) G. R. Desiraju, *Acc. Chem. Res.* **1991**, *24*, 290–296.

[11] a) C. A. Hunter, J. K. M. Sanders, *J. Am. Chem. Soc.* **1990**, *112*, 5525–5534; b) C. A. Hunter, *Chem. Soc. Rev.* **1994**, *23*, 101–109.

[12] The intermolecular noncovalent bonds responsible for the self-assembly of the catenanes of the type described in this paper remain evident in the solution and solid-state structures of the interlocked molecular compounds. See: a) P. R. Ashton, T. T. Goodnow, A. E. Kaifer, M. V. Reddington, A. M. Z. Slawin, N. Spencer, J. F. Stoddart, C. Vicent, D. J. Williams, *Angew. Chem. Int. Ed. Engl.* **1989**, *28*, 1396–1399; b) P. L. Anelli, P. R. Ashton, R. Ballardini, V. Balzani, M. Delgado, M. T. Gandolfi, T. T. Goodnow, A. E. Kaifer, D. Philp, M. Pietraszkiewicz, L. Prodi, M. V. Reddington, A. M. Z. Slawin, N. Spencer, J. F. Stoddart, C. Vicent, D. J. Williams, *J. Am. Chem. Soc.* **1992**, *114*, 193–218; c) D. B. Amabilino, P. R. Ashton, C. L. Brown, E. Córdova, L. A. Godínez, T. T. Goodnow, A. E. Kaifer, S. P. Newton, M. Pietraskiewicz, D. Philp, F. M. Raymo, A. S. Reder, M. T. Rutland, A. M. Z. Slawin, N. Spencer, J. F. Stoddart, D. J. Williams, *ibid.* **1995**, *117*, 1271–1293; d) P. R. Ashton, L. Pérez-García, J. F. Stoddart, A. J. P. White, D. J. Williams, *Angew. Chem. Int. Ed. Engl.* **1995**, *34*, 571–574.

[13] a) T. T. Goodnow, M. V. Reddington, J. F. Stoddart, A. E. Kaifer, *J. Am. Chem. Soc.* **1991**, *113*, 4335–4337; b) A. Bernardo, J. F. Stoddart, A. E. Kaifer, *ibid.* **1992**, *114*, 10624–10631; c) S. A. Staley, B. D. Smith, *Tetrahedron Lett.* **1996**, *37*, 283–286; d) M. A. Lipton, *ibid.* **1996**, *37*, 287–290.

[14] For an example of a chiral amino-acid resolving machine, see: D. J. Cram, *Angew. Chem. Int. Ed. Engl.* **1988**, *27*, 1009–1020 (Nobel lecture) and references cited therein; for a review on enantioselective and diastereoselective recognition of neutral molecules, see: T. H. Webb, C. S. Wilcox, *Chem. Soc. Rev.* **1993**, *22*, 383–395; for recent reports on enantioselective recognition, see: a) M. J. Crossley, L. G. Mackay, A. C. Try, *J. Chem. Soc. Chem. Commun.* **1995**, 1925–1927; b) F. Gasparrini, D. Misiti, C. Villani, A. Borchardt, M. T. Burger, W. C. Still, *J. Org. Chem.* **1995**, *60*, 4314–4315; c) J. Reeder, P. P. Castro, C. B. Knobler, E. Martinborough, L. Owens, F. Diederich, *ibid.* **1994**, *59*, 3151–3160; d) A. Galan, D. Andreu, A. M. Echavarren, P. Prados, J. De Mendoza, *J. Am. Chem. Soc.* **1992**, *114*, 1511–1512; e) K. S. Jeong, T. Tjivikua, A. Muehldorf, G. Deslongchamps, M. Famulok, J. Rebek, Jr., *ibid.* **1991**, *113*, 201–209; f) T. H. Webb, H. Suh, C. S. Wilcox, *ibid.* **1991**, *113*, 8554–8555; g) J. I. Hong, J. K. Namgoong, A. Bernardi, W. C. Still, *ibid.* **1991**, *113*, 5111–5112.

[15] For a more detailed discussion about topological stereochemistry, see: a) D. M. Walba, *Tetrahedron* **1985**, *41*, 3161–3212; b) J.-C. Chambron, C. Dietrich-Buchecker, J.-P. Sauvage, *Top. Curr. Chem.* **1993**, *165*, 131–162. An achiral molecule with nonplanar topology has been synthesized and characterized recently; see c) C.-T. Chen, P. Gantzel, J. S. Siegel, K. Baldridge, R. B. English, D. M. Ho, *Angew Chem. Int. Ed. Engl.* **1995**, *34*, 2657–2660.

[16] A topologically chiral [2]catenane has been synthesized successfully by Sauvage and coworkers and resolved into its two enantiomers by chiral HPLC. See: a) J.-C. Chambron, D. K. Mitchell, J.-P. Sauvage, *J. Am. Chem. Soc.* **1992**, *114*, 4625–4631; b) Y. Kaida, Y. Okamoto, J.-C. Chambron, D. K. Mitchell, J.-P. Sauvage, *Tetrahedron Lett.* **1993**, *34*, 1019–1023.

[17] P. R. Ashton, I. Iriepa, M. V. Reddington, N. Spencer, A. M. Z. Slawin, J. F. Stoddart, D. J. Williams, *Tetrahedron Lett.* **1994**, *35*, 4835–4838.

[18] M. V. Reddington, J. F. Stoddart, unpublished results.

[19] a) D. B. Amabilino, P. R. Ashton, J. F. Stoddart, M. S. Tolley, D. J. Williams, *Angew Chem. Int. Ed. Engl.* **1993**, *32*, 1297–1301; b) D. B. Amabilino, P.-L. Anelli, P. R. Ashton, G. R. Brown, E. Córdova, L. A. Godínez, W. Hayes, A. E. Kaifer, D. Philp, A. M. Z. Slawin, N. Spencer, J. F. Stoddart, M. S. Tolley, D. J. Williams, *J. Am Chem. Soc.* **1995**, *117*, 11142–11170.

[20] A small part of the work described in this paper has been the subject of a preliminary communication: M. Asakawa, C. L. Brown, D. Pasini, J. F. Stoddart, P. G. Wyatt, *J. Org. Chem.* **1996**, *61*, 7234–7272.

[21] P. R. Ashton, C. L. Brown, E. J. T. Chrystal, T. T. Goodnow, A. E. Kaifer, K. P. Parry, A. M. Z. Slawin, N. Spencer, J. F. Stoddart, D. J. Williams, *Angew. Chem. Int. Ed. Engl.* **1991**, *30*, 1039–1042.

[22] The synthesis of this cyclophane has been already published by Hünig et al.; see a) M. Buhner, W. Geuder, W.-K. Gries, S. Hünig, M. Koch, T. Poll, *Angew. Chem. Int. Ed. Engl.* **1988**, *27*, 1553–1556, and for similar work: b) W. Geuder, S. Hünig, A. Suchy, *Tetrahedron* **1986**, *42*, 1665–1677.

[23] The use of a ferrocene-based template has recently proved to be useful for the template-directed synthesis of cyclobis(paraquat-4,4′-biphenylene). See a) P. R. Ashton, S. Menzer, F. M. Raymo, G. K. H. Shimizu, J. F. Stoddart, D. J. Williams, *J. Chem. Soc. Chem. Commun.* **1996**, 487–490; b) M. Asakawa, P. R. Ashton, S. Menzer, F. M. Raymo, J. F. Stoddart, A. J. P. White, D. J. Williams, *Chem. Eur. J.* **1996**, *2*, 877–893.

[24] a) H. Brunner, H. Schiessling, *Angew. Chem. Int. Ed. Engl.* **1994**, *33*, 125–126; b) K. Weil, W Kuhn, *Helv. Chim. Acta* **1944**, *27*, 1648–1669; c) D. J. Cram,

R. C. Hegelson, S. C. Peacock, L. J. Kaplan, L. A. Domeier, P. Moreau, K. Koga, J. M. Mayer, Y. Chao, M. G. Siegel, D. H. Hoffman, G. D. Y. Sogah, *J. Org. Chem.* **1978**, *43*, 1930–1946 and references cited therein.

[25] Stability toward racemization has been tested for the model compound 2,2'-binaphthol. See ref. [24c].

[26] P. R. Ashton, E. J. T. Chrystal, J. P. Mathias, K. P. Parry, A. M. Z. Slawin, N. Spencer, J. F. Stoddart, D. J. Williams, *Tetrahedron Lett.* **1987**, *28*, 6367–6370.

[27] See, for example, the self-assembly of olympiadane: D. B. Amabilino, P. R. Ashton, A. S. Reder, N. Spencer, J. F. Stoddart, *Angew. Chem. Int. Ed. Engl.* **1994**, *33*, 1286–1290.

[28] P. R. Ashton, M. Blower, D. Philp, N. Spencer, J. F. Stoddart, M. S. Tolley, R. Ballardini, M. Ciano, V. Balzani, M. T. Gandolfi, L. Prodi, *New. J. Chem.* **1993**, *17*, 689–695.

[29] The different sizes of crown ethers **BPP34C10** and **1,5DN38C10** have been used in the controlled self-assembly of a [3]rotaxane incorporating three constitutionally different components. See: D. B. Amabilino, P. R. Ashton, M. Bělohradský, D. Philp, F. M. Raymo, J. F. Stoddart, *J. Chem Soc. Chem. Commun.* **1995**, 751–752.

[30] The kinetic and thermodynamic data were calculated by two procedures: a) the *coalescence method*, where values for the rate constant k_c at the coalescence temperature (T_c) were calculated (I. O. Sutherland, *Annu. Rep. NMR Spectrosc.* **1971**, *4*, 71–235) from the approximate expression $k_c = \pi(\Delta\nu)/(2)^{1/2}$, where $\Delta\nu$ is the limiting chemical shift difference (Hz) between the coalescing signals in the absence of exchange; b) the *exchange method*, where values of k_{ex} were calculated (J. Sandström, *Dynamic NMR Spectroscopy*, Academic Press, London, **1982**, Ch. 6) from the approximate expression $k_{ex} = \pi(\Delta\nu)$, where $\Delta\nu$ is the difference (Hz) between the line width at a temperature T_{ex}, where exchange of sites is taking place, and the line width in the absence of exchange. The Eyring equation was subsequently employed to calculate $\Delta G_c^{\ddagger}$ or $\Delta G_{ex}^{\ddagger}$ values at T_c or T_{ex}, respectively.

[31] For a more detailed discussion about the "rocking" process—that is, the equilibrations of the protons attached to the included hydroquinone rings between positions where they are directed toward the center of the *p*-phenylene ring in the *p*-xylyl spacer of the cyclophane and positions where they protrude outside the π-electron-deficient cavity—see: a) ref. [12c]; b) P. R. Ashton, J. A. Preece, J. F. Stoddart, M. S. Tolley, D. J. Williams, *Synlett* **1994**, 1063–1066.

[32] Compound (*R*)-**23**·4Cl was obtained by adding a saturated solution of $(n\text{Bu})_4\text{NCl}$ in Me_2CO to a solution of (*R*)-**23**·4PF_6 in Me_2CO until no further precipitation occurred.

[33] The crystal structure of the 1:1 complex between cyclobis(paraquat-*p*-phenylene) and 2-methylindole is discussed in: P.-L. Anelli, M. Asakawa, P. R. Ashton, R. A. Bissell, G. Clavier, R. Górsky, A. E. Kaifer, S. J. Langford, G. Mattersteig, S. Menzer, D. Philp, A. M. Z. Slawin, N. Spencer, J. F. Stoddart, M. Tolley, D. J. Williams, *Chem. Eur. J.* **1997**, *3*, in press.

[34] See, for example, refs. [12] and [23].

[35] K. A. Connors, *Binding Constants*, Wiley, New York, **1987**.

[36] *N*-Acetyl-D-tyrosine was prepared according to V. Du Vigneaud, C. E. Meyer, *J. Biol. Chem.* **1933**, *97*, 295–308.

[37] Macromodel V5.0: F. Mohamadi, N. G. J. Richards, W. C. Guida, R. Liskamp, M. Lipton, C. Caufield, G. Chang, T. Hendrickson, W. C. Still, *J. Comput. Chem.* **1990**, *11*, 440–467.

[38] For a discussion on [CH···π] interactions, see: M. Nishio, Y. Umezawa, M. Hirota, Y. Takeuchi, *Tetrahedron* **1995**, *51*, 8665–8701 and references cited therein.

[39] M. Asakawa, P. R. Ashton, S. E. Boyd, C. L. Brown, R. E. Gillard, O. Kocian, F. M. Raymo, J. F. Stoddart, M. S. Tolley, A. J. P. White, D. J. Williams, *J. Org. Chem.* **1997**, *62*, 26–37.

[40] Spartan V4.1, Wavefunction, 18401 Von Karman Ave., 370 Irvine CA 92715, USA.

[41] For a recent example of chemistry carried out on rotaxanes, see: R. Jäger, M. Händel, J. Harren, K. Rissanen, F. Vögtle, *Liebigs Ann.* **1996**, 1201–1207.

[42] B. S. Furniss, A. J. Hannaford, P. W. G. Smith, A. R. Tatchell, *Practical Organic Chemistry*, Longman, New York, **1989**.

[43] a) N. Maigrot, P. Mazaleyrat, *Synthesis* **1985**, 317–320; b) T. Hayashi, K. Hayashizaki, T. Kiyoi, Y. Ito, *J. Am. Chem. Soc.* **1988**, *110*, 8153–8156.

[44] W. Weener, *J. Org. Chem.* **1952**, *17*, 523–528.

[45] Crystallographic data (excluding structure factors) for the structures reported in this paper have been deposited with the Cambridge Crystallographic Data Centre as supplementary publication no. CCDC-100084. Copies of the data can be obtained free of charge on application to The Director, CCDC, 12 Union Road, Cambridge CB21EZ, UK (Fax: Int. code +(1223)336-033; e-mail: deposit@chemcrys.cam.ac.uk).